

The effect of modeling lateral stiffness of pile foundations on numerical analyses of structural frames

Tiago de Souza Magnus

School of Engineering

Thesis submitted for examination for the degree of Master of Science in Technology.

Espoo 27.08.2018

Supervisor

Prof. Jari Puttonen

Advisors

Mr. Hannu Uusitalo, M.Sc

Mr. Juha Valjus, M.Sc

Copyright © 2018 Tiago de Souza Magnus



Author Tiago de Souza Magnus

Title The effect of modeling lateral stiffness of pile foundations on numerical analyses of structural frames

Degree programme Building Technology

Code CE.thes

Supervisor Prof. Jari Puttonen

Advisors Mr. Hannu Uusitalo, M.Sc, Mr. Juha Valjus, M.Sc

Date 27.08.2018

Number of pages 72+13

Language English

Abstract

Nowadays in Finland, there is an increasing interest in relying on the lateral resistance of pile foundation with less usage of raking piles. However, there is a current lack of understanding of soil-structure interaction and the cooperation between structural and geotechnical engineers is ineffective, which makes it difficult to fully rely on the current results. Therefore, this study was carried out to assess the effects of modeling lateral stiffness of pile foundation on structural stability analysis. Additionally, a general overview of soil-structure interaction and a suggestion of improved cooperation between the two engineering fields are provided in this work.

The analysis was carried out on a building frame with four different lateral stiffness models on the foundation, the goal was to measure the response of the building frame to the models. The results show that the deformations of the building and foundation as well as the load distribution on the foundation and on the load bearing structure were sensible to the stiffness of the foundation.

It has been concluded from the results that it is important to have a precise lateral stiffness model in order to have a more realistic load distribution on the load bearing structure, and that soil analysis should be carried out accordingly to the deformations obtained on the structural stability analysis. In order to achieve this goal, it is necessary to reinforce the cooperation between structural and geotechnical engineers in the exchange of information and the check of results throughout the design process. By doing this, both soil and structural analysis can be carried out with more precision and reliability of results can be increased.

Keywords Foundation, Pile, Structural analysis

Contents

Abstract	3
Contents	4
Abbreviations	6
1 Introduction	7
2 Collaboration between structural and geotechnical designer	9
2.1 Typical collaboration in Finnish design offices	9
2.2 Optimal Collaboration between structural and geotechnical engineering	11
3 Horizontal forces affecting frame	12
3.1 Wind actions	12
3.2 Structural imperfections	14
4 Soil-Structure Interaction (SSI) model in structural engineering	15
4.1 General overview	15
4.2 Soil response under different types of loading	16
4.2.1 Soil behavior under cyclic loading	17
4.2.2 Consideration of soil as an approximated linear behavior	20
4.3 Typical FEM structural model for SSI analysis	21
5 Estimating pile capacity	23
5.1 General pile behavior and limiting pressure	23
5.1.1 Limiting lateral pressure: non-cohesive soils	26
5.1.2 Limiting lateral pressure: cohesive soils	26
5.2 General theory of elasticity for piles	27
5.3 P-y curve: a non-linear method	28
5.4 Subgrade reaction approach	29
5.4.1 Non-cohesive soils	29
5.4.2 Cohesive soils	30
5.4.3 FEM spring model for non-cohesive soils	31
5.4.4 FEM spring model for cohesive soils	32
6 Pile groups	33
6.1 General pile group theory	33
6.2 Introduction to p-multiplier in group interaction	34
6.3 Experimental researches on the p-multipliers	35
6.4 Implementation of equation for modified pile spacing	37
6.4.1 Pile efficiency factor for pile groups by Reese (2006) [22]	37
6.4.2 Pile row efficiency factor by Rollins et al (2006) [25]	39
6.4.3 Pile row efficiency factor by Al-Shamary et al (2018) [1]	40
6.5 Summary of results	41

7	Methodology of the analysis	44
7.1	Structural model and considerations	44
7.1.1	Vertical loadings	44
7.1.2	Wind loading	45
7.1.3	Loading combinations and analysis type	45
7.2	Defining pile distribution and pile group geometry	45
7.3	Soil type and soil-pile analysis	47
7.3.1	Soil type	47
7.3.2	Subgrade reaction approach	48
7.3.3	P-y method	48
7.4	Pile group efficiency	50
7.5	Soil-foundation stiffness models	50
7.5.1	Model 1: Simply supported	51
7.5.2	Model 2: Subgrade reaction approach with no effects of pile group	51
7.5.3	Model 3: Based on p-y analysis with 100 cycles	53
7.5.4	Model 4: Based on a simplification of Model 3	54
8	Results and discussion	56
8.1	Modeling time	56
8.2	Availability of results for piles	56
8.3	Other comments concerning modeling and results	58
8.4	Deformations at foundation level	58
8.5	Variation on pile loads	59
8.6	Lateral loading	61
8.7	Top floor deformations	62
8.8	Loading distribution on shear walls	63
8.9	Natural frequency	64
9	Conclusion	66
9.1	Applications of the Models	67
9.2	Cooperation between structural and geotechnical engineers	68
9.3	Final comments	69
	References	70
A	Annex 01	73
B	Annex 02	74
C	Annex 03	75
D	Annex 04	80
E	Annex 05	83
F	Annex 06	85

Abbreviations

FEM	Finite Element Method
SLS	Serviceability Limit State
ULS	Ultimate Limit State
EN	European Standard
SSI	Soil-Structure Interaction
kN	Kilo Newton
MPa	Mega Pascal

1 Introduction

Foundations are components placed between the superstructure and the soil in order to transfer loads from the superstructure without over-stress the soil stratus. Foundations can be divided into *shallow foundations* and *deep foundations*. Shallow foundations can be generalized as footing elements laying over a layer of soil with enough capacity to carry the imposed loads. Whereas, when the resistant layer of soil is not found close to the surface, deep foundations need to be used in order to transfer the loads to a deeper and more resistant level, sometimes even to a bed-rock. One example of deep foundations is the pile foundation. [7]

Piles are slender elements used to transfer loads from foundations to a layer of bearing resistant soil or bed rock. Piles may be made of concrete, steel, wood or a composite of steel and concrete. The vertical loads can be transferred to the soil by contact friction along the pile shaft, directly to a hard layer of soil by the end of the pile (end-bearing piles) or a combination of both. [7], [8]

Most of the pile foundations are subjected to horizontal loading, which are generally smaller than vertical loads. These loads can, in most of the cases, be taken by the group of vertical piles by lateral resistance, which is a problem that involves the interaction between the soil and the structure. However, until the middle of the twentieth century, engineers did not have enough expertise on how to evaluate lateral resistance of vertical piles, so it was supposed that piles resisted only axial to loads and horizontal loads were taken by piles with an angle, which are named raking or batter piles. These raking piles provide enough horizontal resistance due to its axial resistance acting in the horizontal direction and are also loaded by bending. [11], [22]

Although raking piles are still a good design solution for a range of projects, their utilization, ignoring the lateral resistance of the soil, is a conservative model and of higher costs [11]. Raking piles are also more demanding and not as efficient as installing vertical piles [8]. For example, alignment standards limit deviation of the center line from design to 1:25 compared to 1:75 for a normal pile [11], and where the angle of inclination goes over 4:1, installation on site may require special equipment, which elevates its costs. Rough estimations were carried out and it shows that it is from 5% to 15% more expensive to use a raked pile than a normal pile. Moreover, in foundations with a relatively high density of vertical piles it becomes very difficult to place the raked piles due to the lack of horizontal space.

Because of the need to create more economical structures and also due to the difficulties when using raking piles in projects, engineers are starting to be more interested in taking into account the lateral resistance of a vertical pile group [8]. However, the current reality in engineering offices in Finland is that structural engineers do not have enough information of soil-structure interaction to totally rely on the horizontal resistance of foundations under lateral loads. Moreover, there is also a lack of understanding of soil-structure interaction and how this should be handled with

geotechnical offices, which leaves geotechnical engineers with an open choice of which data and in what format it will be sent to structural offices. The result of this is the uncertainty if the current lateral stiffness of foundations being applied in the stability models is presenting good accuracy. There exists also the uncertainty of how piles behave within a group and how their geometries affect the overall resistance. These problems are increased specially in higher buildings. Consequently, raking piles are still largely used in engineering solutions.

It is known that accurate models for soil-structure interaction are already developed and are complete and exact to some extent. However, these models are relatively complex and require time and accurate soil investigation, which is not always available for daily engineering offices when dealing with typical structures. Therefore, the remaining problem is not how to estimate a precise lateral stiffness and capacity for the foundation, but how to model the foundation stiffness for the structural analysis in terms of spring distribution. For this reason, this study focuses on simplifications of complex theories in order to introduce the topic to engineers not familiar with soil-structure interaction. Therefore, the goal of this study is to explain the basic principles of soil-structural interaction, verify and suggest pile-group stiffness models and analyze the structural sensitiveness due to the variation of how soil-foundation stiffness is modeled. The soil-foundation stiffness models were chosen from a very simple model to a relatively complex. As a result, the target was to improve interaction between structural and geotechnical engineers in order to produce better work and suggest pile group efficiency when full group results are not available. It is worth mentioning that this study does not focus on designing the pile foundations nor improving the methods of estimating soil-structure interaction but it focuses on how to effectively apply its resistance and stiffness in the structural model in order to estimate the structural response and minimize the use of raking piles. The effects in the natural frequency for wind induced vibration will also be calculated to make a comparison, as it is typical to assume a pseudo-static wind load when the structure is not prone to wind induced vibrations.

2 Collaboration between structural and geotechnical designer

Geotechnical Engineering is a subdivision of civil engineering and it takes care of all works related to soil or rock behavior with man-made structures. It can also be divided into two fields, *Soil and rock mechanics* and *Foundation design*. In soil mechanics the goals are to characterize the physical index of the soil, its behavior and capacities, while foundation design is concentrated on designing the various existent types of foundations and soil retainers [7]. The current situation in Finland, which put forth the reasons of this study, is that the overall foundation design is performed by structural engineers while geotechnical engineers characterize the soil resistance for the a chosen foundation. As a result, the overall responsibility of the foundation design quality is over structural engineers, which should then understand which values and results can be trusted.

2.1 Typical collaboration in Finnish design offices

Analyzing the situations that formulated the topic of this research, it was noted that the communication between structural and geotechnical engineering is still impaired, mostly because of lack of instructions from both parts. Meaning that, structural engineers do not specify correctly what information they need for the foundation stiffness model and geotechnical engineers do not specify what information they need from the structural model in order to give back appropriate soil-foundation results. This leads to speculations from both parties.

While geotechnical offices do not get any specifications of what kind of results they should send back or what are the limitations and considerations from the side of the structural model, they are free to choose what information and in what format they will send to structural offices. The most results received by structural offices are a force resistance per pile or per pile group, sometimes with a maximum deflection. However, it is not well specified what were the considerations taken into account when obtaining those results, such as: what soil-pile analysis was set (static, cyclic, dynamic), what was the nature of the load used in the analysis (static, sustained, cyclic) and if that is the ultimate load resistance or if it is just a limit resistance set by the office. In the other hand, these pieces of information are never asked and the data received in structural offices are applied in stability models even though the nature of the results are unknown. This lack of understanding of the principles used in describing soil parameters may decrease considerably the reliability of stability analyses of the structure carried out by the FEM.

The issue goes to other levels when working with pile groups. As the overall resistance of the group is dependent on the pile type, group geometry and pile spacing (see chapters 5 and 6), structural offices need to send it to geotechnical design. However, at this early stage it is not possible for structural engineers to provide precise di-

mensions for the pile groups as the geometry depends on the force arriving at the foundation from the structure in relation with the soil resistance. The solution is then to guess a geometry for a pile group and send it to geotechnical design, which later on, will send back an overall force resistance for the pile group. In this study, this preliminary geometry of a pile group is called as a *standard block*).

Let us consider now how to introduce this force resistance into the model. It cannot be set as a force or a rigid support because the structure and the force distribution is dependent on the deformations at foundation level. Therefore, how to transform this force value to a soil-foundation model which will allow deformation and simulate the soil stiffness? The solution normally used is to calculate a single spring at the top of the foundation block (see Figure 1) by utilizing Hook's law (equation (1)), where vertical loads are normally considered to be taken by compression/traction in the piles and the flexibility in the vertical direction would be the same as the flexibility of the piles.

$$F = k * \Delta x \quad (1)$$

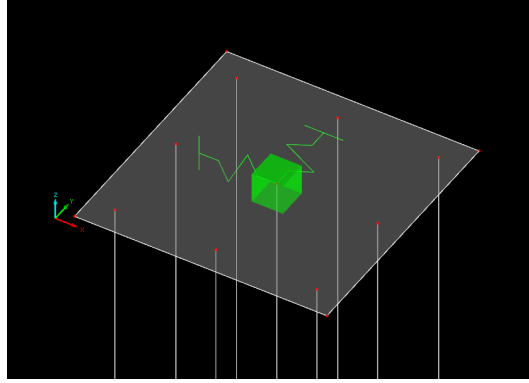


Figure 1: Spring in foundation cap.

However, after inserting the *standard block* into the model, the distribution of reaction forces might change, creating new needs for some pile groups. For instance, how to estimate the resistance of another geometry of pile group when the load imposed by the structure differs in a great amount from the standard block resistance? The answer for this question is to send back the geometries to the geotechnical office and get the right resistance for each geometry. Unfortunately, this is not what happens since interaction between both fields are not planned to happen in later stages of the project. Consequently, the resistance of the new block is then based on educated guesses and to reduce the level of uncertainties, solutions such as the use of raked piles are largely used.

2.2 Optimal Collaboration between structural and geotechnical engineering

Some insights of an improved collaboration between both engineering fields were found along this research, however, large part of the recommendations stated here are based on a report made to the National Institute of Standards and Technology (NIST) [30] in USA. The report brings some insights on how both fields should work together, and states that increasing the amount of collaboration between both parties appears to be beneficial, as well as understanding each other's field, needs and whys, can be an important point in collaboration and on the project.

It is important as well that both fields have at least a general idea of soil-structure interaction, which would develop a wider understanding of soil and structural needs making work between parties flow easier. Geotechnical engineers should also be part of meetings were they can share ideas and make sure their recommendations are being followed. Design meetings should be performed between both fields in order to exchange needs of data and create a more iterative design process.

Both fields should understand that by modeling a accurate soil-foundation stiffness in the model a more realist load distribution and displacement is generated and gives additional insight in the foundation design. Therefore, Geotechnical design should not be considered as finished before foundation design is done. It is also important to mention that a load distribution estimation would help geotechnical engineers to reach a more precise result with less interactions.

The use of a checklist from both fields can overcome some lacks or noneffective exchange of information. Although each project has its own needs, a checklist would help to pass forward some initial requests from both fields. Such checklist could contain basic standard information needed by both fields, as well as design and modeling recommendations.

3 Horizontal forces affecting frame

Actions are very important factors and need to be analyzed carefully when idealizing a structural model. They should not be excessively minimized or neglected, so that the structure will not be compromised, and they should also not be excessively overestimated so that it will not lead to unnecessary structural sections and possibly cause design challenges that can be avoided when utilizing the correct solicitations. Accordingly to EN 1990 [31], loads can be classified in 3 different ways, such as:

- Permanent actions (G);
- Variable actions (Q);
- Accidental Actions (A).

Where the permanent actions stands for the self-weight of the structure and other permanently installed equipment; the variable actions comprehend the dynamic actions such as wind and moving loads and the accidental actions are the unexpected charges such as explosions, seismic activities and impacts of external elements (cars, buses and trucks).

Loads are acting in several different ways over a structure, however, for the purpose of this work only the horizontal charges will be discussed; as vertical loads and how they are taken by the foundation is not the object of this research. The horizontal actions of most importance for this research are:

- Wind pressure;
- Imposed lateral loads;
- Soil pressure;
- Structural imperfections.

These loads are transferred along the structure until the foundation where it needs to be transferred to an element of support, normally soil. The support reaction for these horizontal loads reaching the foundation can be generated by direct soil pressure/resistance (when it has capacity) or by raking piles that transfer horizontal loads directly to rigid foundation (bed rock).

3.1 Wind actions

Wind actions can be generalized as surface pressure applied on the external elements of a structure or on internal elements of open structures. Moreover, when large areas are swept by wind, tangential friction forces might be significant [6], [34]. Accordingly to EN 1991-1-4 and EN 1990, its actions can be represented by a simplified set of pressure or loads whose effects represent the extreme effects of the turbulent wind

and classified as variable actions unless otherwise specified [31], [34].

Wind loads are the most critical case for lateral loads in most structures and it is worth mentioning that it is important to estimate wind loads as precisely as possible, since an overestimation of loads would create unnecessary bigger stiffening systems and foundation elements leading to a more expensive structure; and underestimated wind loads could bring the structure to collapse during its utilization period due to a lack of resistance. EN 1991-1-4 mentions that wind tunnel tests and/or a proven and validated numerical method may be used as a supplement to the Eurocode calculation standard, as well as specific local data may be found in national annexes [34].

Even though wind loads are typically modeled as static loads in the stability model, they can often be characterized as cyclic loading of foundations. At foundation level, cyclic loads may degrade soil capacity and increase soil movements [16]. Over the foundation level, this cyclic effect might be of particular importance for high and flexible structures which are prone to wind induced oscillations. Figure 2 illustrate the cyclic nature of wind loads, which can be explained by the fact that wind hits the building repeatedly over the time and from all directions, this will make the foundation be loaded from one direction in a certain period of time and loaded from the opposite direction in a later period of time. The loading is released when wind stops blowing but the process may happen several times along the lifetime of the building which will create a cyclic loading at the foundation. [15]

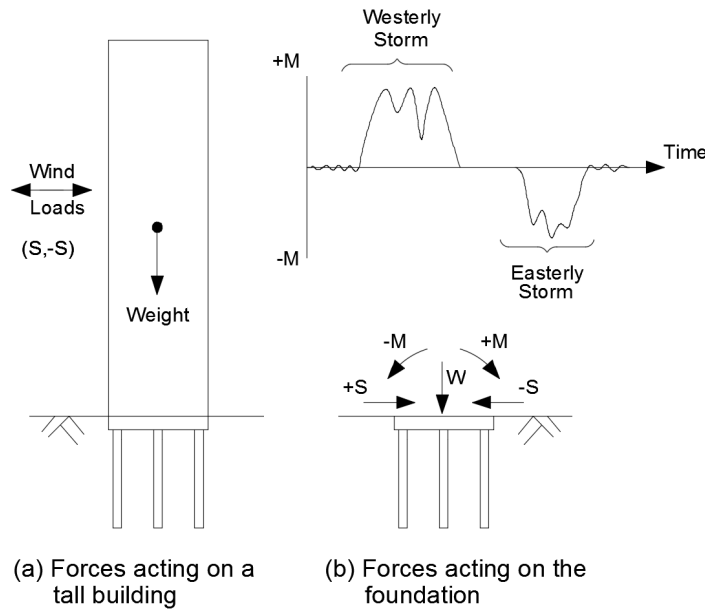


Figure 2: Cyclic loading due to wind load [15].

3.2 Structural imperfections

Generally, structures are prone to have small imperfections due to its construction process, which are not faults, but a natural consequence of man-made work. Such imperfections might be due to deviations in the geometry of form-work or deviations in the vertical alignment of the elements. Imperfections are limited by codes, such as EN13670 for concrete structures. For this study it is worth mentioning the imperfections in alignment of columns over the height of the structure. As demonstrated in Figure 3, projecting the axial force of a tilted column with a rotation imperfection θ produce a horizontal force F_x on the node, such deviations are worth to be taken into account in the calculation model. In high flexible structures wind forces can also tilt the structure causing imperfections and may also generate the same effects.

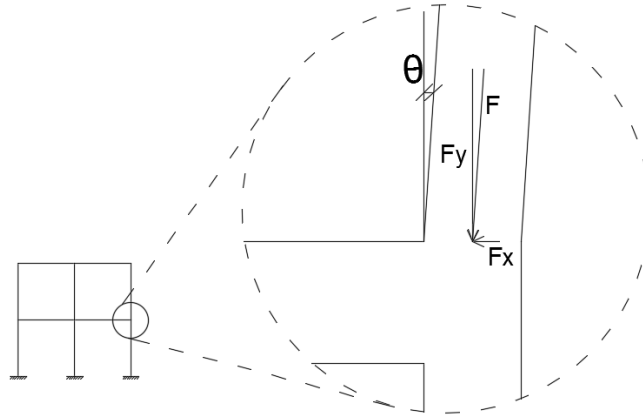


Figure 3: Structural imperfection.

4 Soil-Structure Interaction (SSI) model in structural engineering

Most problems associated with SSI application comes from poor understanding of its fundamental principles [30], where structural engineers are not familiar with the topic, communication with the geotechnical designer becomes difficult and a set of uncertainties rise in the design. Accordingly to Edgers et. al. (2005) [9], modeling the foundation and the deformable soil with the structure is an important factor to capture the effects of SSI on the structural response and this requires a good coordination between structural and geotechnical engineer. Therefore, the goal of this chapter is to give a general overview of SSI so that engineers are familiar with the problems encountered in this field.

4.1 General overview

In order to understand the general way in which SSI affects structural analysis, let us consider the system presented in Figure 4, where the force F applied on the mass m represents the building laterally loaded. If considered a rigid support (Figure 4 (a)) the total deflection would be calculated as simple as presented in Equation 2, where k is the stiffness of the building. However, when considering a flexible support (Figure 4 (b)) with vertical k_z , horizontal k_x and rotational springs k_{yy} , the deflection would change to a larger value dependent on the properties of each spring, as shown in Equation 3. [30]

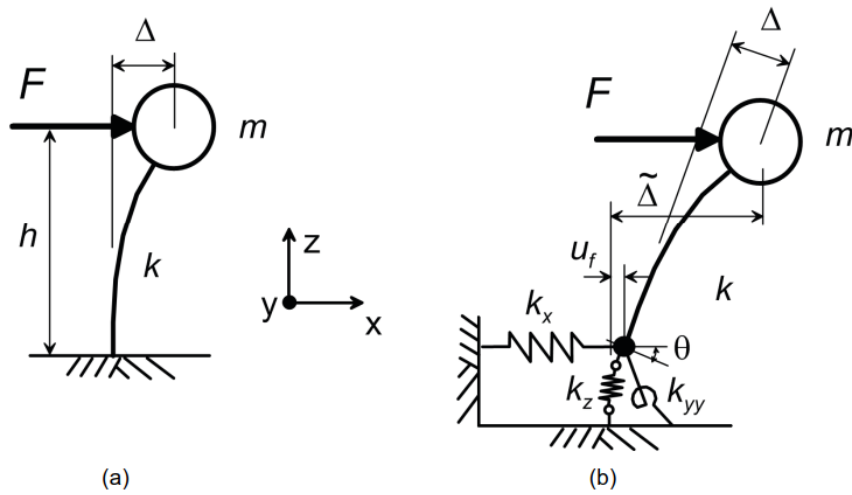


Figure 4: Illustration of deflection in stiff and flexible supports [30].

$$\Delta = \frac{F}{k} \quad (2)$$

$$\tilde{\Delta} = \Delta + u_f + \theta h \longrightarrow \frac{F}{k} + \frac{F}{k_x} + \left(\frac{Fh}{k_{yy}} \right) h \quad (3)$$

It is concluded, from a structural frame point of view, that the flexibility of foundation affects the results of the frame on top of it. In the other hand, as soil is not a perfect elastic material, the level and nature of the pressure imposed over the soil by the structure can change its characteristics. Therefore, both soil and structure are interdependent and should not be analyzed separately. Understanding this allow us to think of factors playing a role in SSI, such as how the soil behaves to different types of loads and deflections, which soil analysis is appropriate for the different design, and later to how we set the structural model for global analysis.

4.2 Soil response under different types of loading

Besides the natural characteristic of the soil, which will define its own behavior, the nature of the loading can also affects soil response. Common loading types can be classified as: short term static, sustained, repeated and dynamic. [22]

Dynamic loading includes seismic events and loads from vibrating machines installed on the structure [22]. Seismic actions will create additional lateral forces in the structure increasing lateral soil motion. These effects can be induced in the foundation by inertial interaction between the structure and soil damping or by kinematic interaction by the soil movement on the pile shaft. Loads which are dynamic in nature increase the risk of resonance in the structural system, which are dependent on some factors including the period of the loading, period of the structure, stiffness and damping of foundation system. [16], [30]. In some cases, specially in high-rise buildings, wind load needs to be considered as of dynamic nature due to its high influence in the building structural response, however, these analyzes are not in the scope of this work and therefore will not be further explained.

Effects of short-term static loading can be directly estimated from the properties of supporting soil. Although short-term static load hardly happens in real structures, static load analysis can be used when allowable deflections are small and if the soil is granular or an over-consolidated clay. However, if sustained loading is applied to a supporting soil of soft to medium clay, consolidation can be expected and needs to be taken into account. [22]. Effects of short term static loading can be estimated by using the *p-y method* or *subgrade reaction approach*, both explained in Sections 5.3 and 5.4 of this work.

Lastly, repeated and cyclic loading, which normally occur against offshore structures or in structures exposed to wind loads, is a problem that demands careful consideration and analysis. If deflections are small, where soil is acting in a linear fashion, the same

soil analysis and limitations used for static loading can be applied. However, for larger deflections, significant loss of resistance can occur in over-consolidated clay and in some granular soils. If deflections are large enough to create large consolidations and a gap between pile and soil, then soil resistance will not be present anymore for smaller deflections and if water is present, soil erosion can be expected as water is squeezed out taking soil particles with it. [22]

4.2.1 Soil behavior under cyclic loading

This study will take into account the reoccurring (cyclic) nature of wind loads, and as soil behavior under cyclic load appears to be highly complex, some of its main characteristics are going to be here explained in order to rise awareness in the structural engineering field so that proper decision can be made when choosing for a cyclic or static analysis.

A soil under cyclic loads is likely to suffer stress reversals due to the stress and release over time. To understand how stress reversals affects soil, consider Figure 5 (a), at every stress release (curves A-B and C-D) there is a change in the strain level, part of it is recovered and another part remains in the soil during stress-release, and therefore, the stress level at any strain value is smaller during the stress-release part than during the stress-increase part, meaning that the soil is not anymore reacting at the same level as the force that has been applied. Figure 5 (b) shows that at after every stress reversal, the stiffness of soil increases drastically for a short moment and then subsequently decreases. [15]

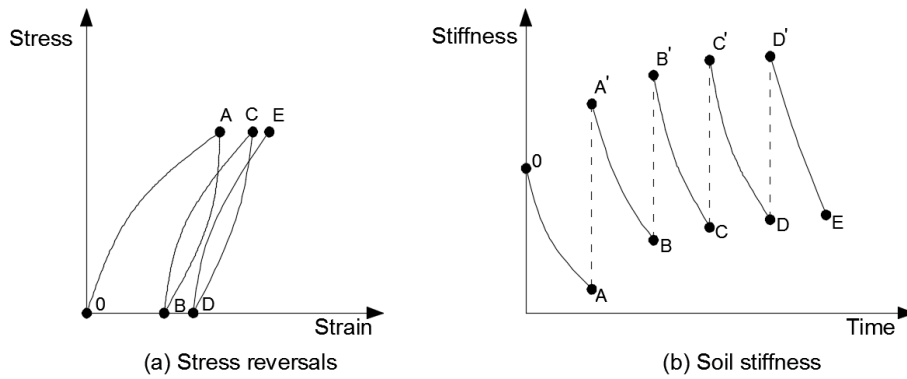


Figure 5: Effects of stress reversals on soil stiffness [15].

Generally speaking, the tendency of soil stiffness is to decrease with loading cycles. To view this more clearly, the work of Snyder (2004) [29], who performed a full scale cyclic load test in a pile group in clay, and Walsh (2005) [38] will be used to explain the effects of cyclic loading on soil-pile interaction.

Pushing the pile to higher and higher deflections, piles presented residual deformations when loading was totally released. A complete plot of cyclic loading and deflection is shown in Figure 6. Snyder (2004) [29] explains that part of this residual deflection

was due to caving of the soil into the gap behind the pile, which prevented it to return to its original position when loading was released.

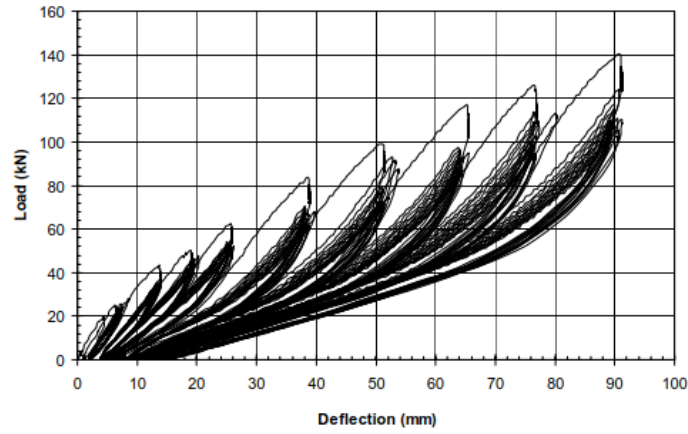


Figure 6: Loading versus deflection [29].

In respect with soil resistance, Walsh (2005) [38] comparing his work with that of Snyder (2004), plotted the loading deflections both for clay and sand to 1 and 10 loading cycles, which can be seen in Figure 7. It is noticeable that for the same loading value deflection increases in higher loading cycles.

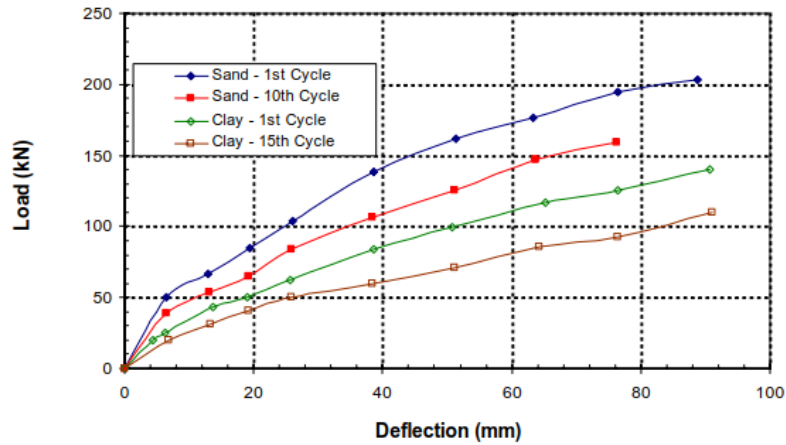


Figure 7: load versus deflection after cycles [38].

Another way we can visualize the reduction of soil resistance is by the normalized soil stiffness presented in Figure 8 for clay and in Figure 9 for sand.

Concerning the gaps that might appear between pile and the surface of the soil, as exemplified in Figure 10, Snyder (2004) [29] states that gaps were possible to be seen and measured until some depth. Figure 11 show a plot of the gap between pile and

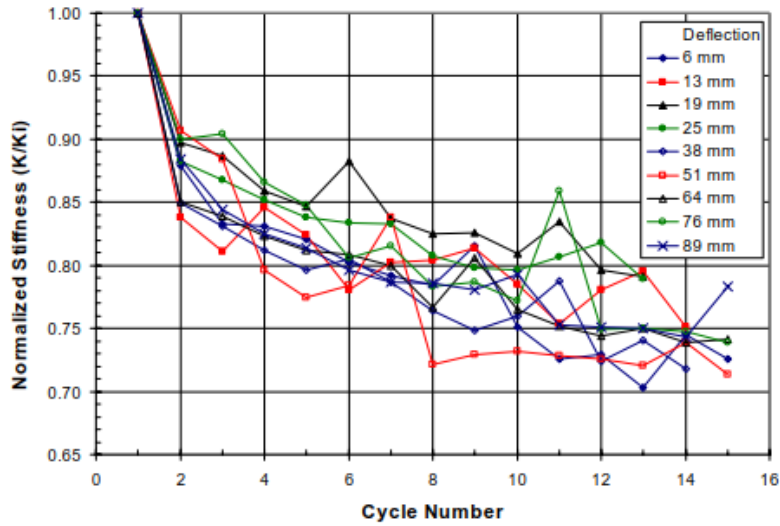


Figure 8: Normalized soil stiffness in clay [29].

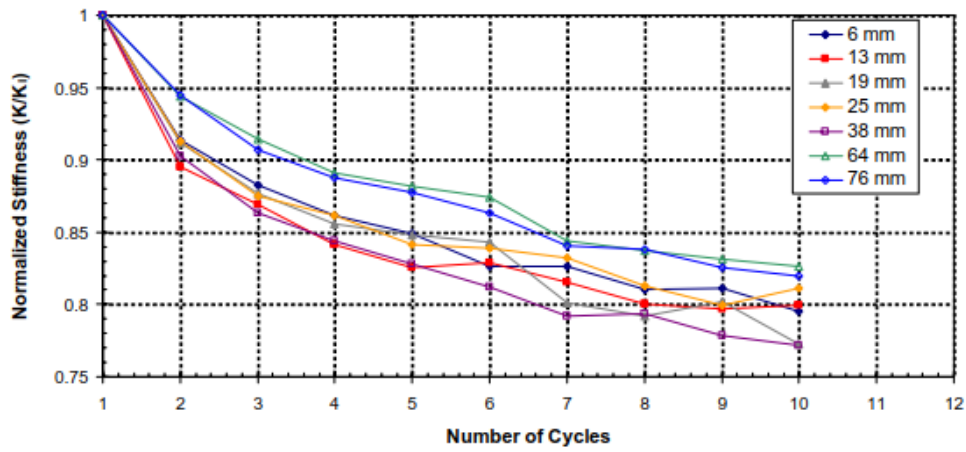


Figure 9: Normalized soil stiffness in sand [38].

clay soil to different deflections measured by Snyder (2004). Whereas in sand, Walsh (2005) states that the gap becomes partially filled by soil after loading release, and therefore, a good measure cannot be done.

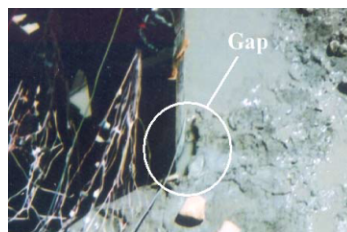


Figure 10: Gap in soil after loading release [29].

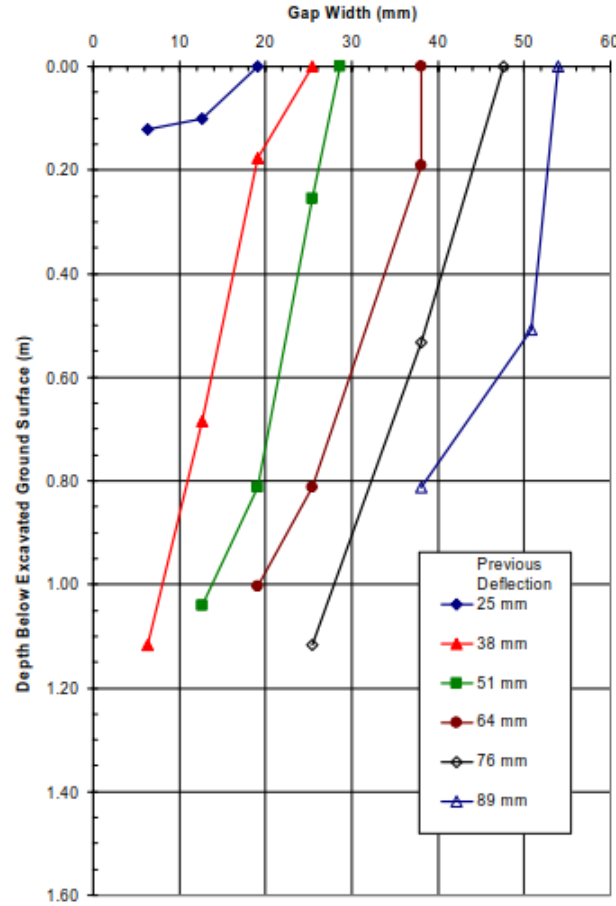


Figure 11: Gap of soil versus deflection [29].

4.2.2 Consideration of soil as an approximated linear behavior

Soil cannot be found as an elastic homogeneous material and any soil that is generalized as behaving elastically is an approximation of its true behavior. However, as matter of practice, linearization or an approximation of it is typically used in many structural analysis.

In practical predictions of lateral load deflection of piles it was a typical practice to use the secant modulus E_{sec} when no yielding is present in the soil, in this case, the soil modulus would decrease as load increases (See Figure 12) [17], [18]. However, the soil response tends to be non-linear and a single secant cannot match the behavior from small loads up to the maximum. If a secant is set for the ultimate limit load it would be too soft to simulate the response of small magnitude loading cycles [18]. A solution could be achieved by selecting trial secant modulus, calculating pile response and correcting the secant modulus until convergence [22].

While linearization of the elasto-plastic behavior of the soil was used in this work, it is extremely important to mention that this approximation was used only for loads

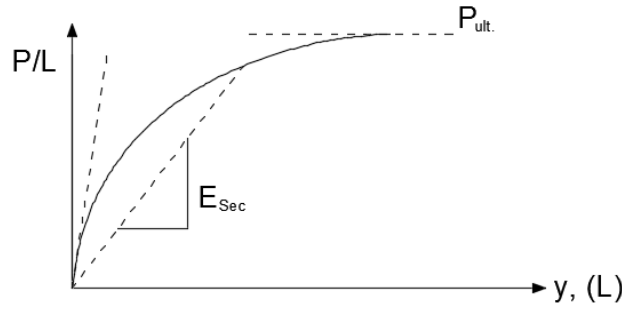


Figure 12: Secant modulus of soil (adapted from [22]).

that can be considered static and limited to small deflections to avoid gapping effects. This practice is not recommended for large deflections when soil presents yielding and gapping or when loading are of dynamic nature.

4.3 Typical FEM structural model for SSI analysis

Typically, structural analysis is performed by using a software based on Finite Element Method (FEM). FEM is a numerical tool that can be used to solve complex mathematical problems described by differential equations, the method follows an idea of dividing a mathematically complex continuous body into small interconnected elements, which will have simpler solutions [20]. FEM allows the assembly of the whole structure in one unique model and calculations are done much faster than, for example, if done by hand methods, and with better accuracy of results. In a typical structural model the continuous building is divided into a series of different elements connected by nodes, beam elements are normally used for columns and beams, plates or shell elements for slabs and walls, and springs or supports with rotational and translation restrains for the element supports.

The final model for soil-structure interaction generally looks like the example in Figure 13. In this model it is considered the real size of the structure and all vertical and horizontal loading. For the foundation it is typical to use springs to simulate the stiffness of the soil-foundation and these springs can be set both in the pile cap (springs A in Figure 13) or along the pile shaft (springs B in Figure 13).

An important consideration when piles are combined with a pile cap is whether or not lateral resistance is provided by the pile cap. Soil might be settle away from shallow foundation elements, specially in cases when soil has been excavated for the casting of the pile cap and filled in afterwards. In such cases, lateral load resistance would be provided only by piles. However, if soil settlement and gapping is not to be expected around pile caps, then a resistance combination could be used between piles and pile cap. [30]

A mistake commonly made today is to think that the loading distribution from the structure to the soil is mainly dependent on the structure. However, it is not entirely

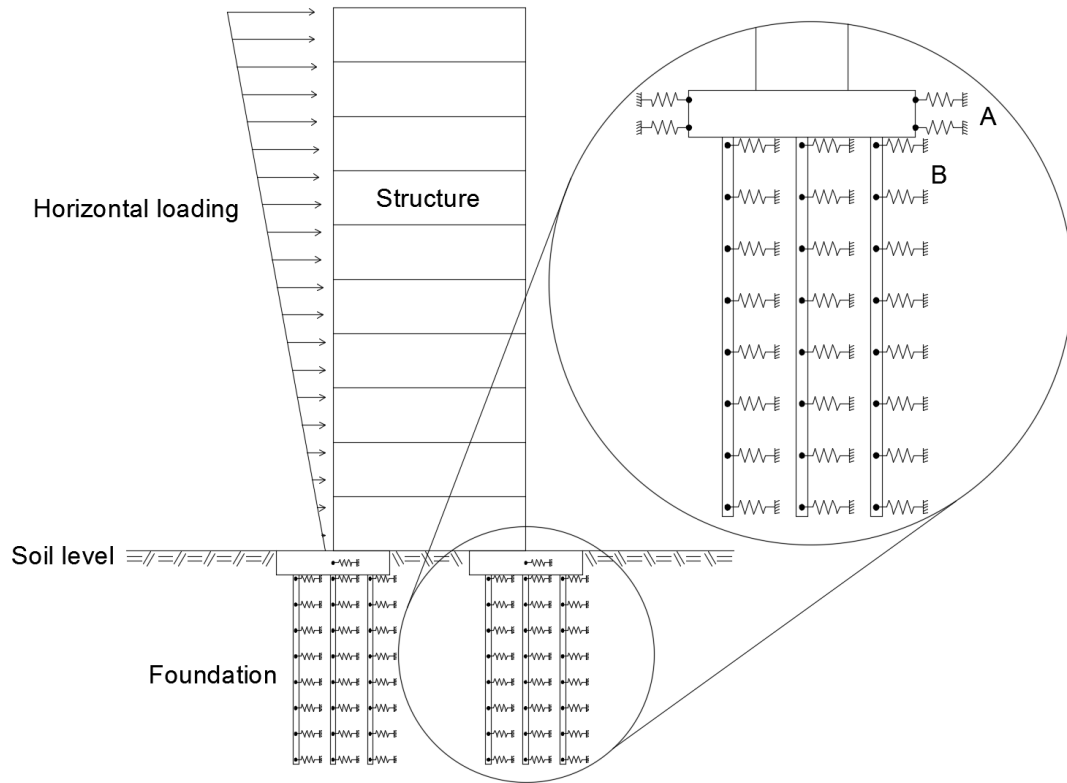


Figure 13: Structural model in FEM software.

like that. The distribution of loads from the structure to the foundation and to the soil is as dependent on the soil-foundation stiffness as it is dependent on the structural system itself. With the foundation deforming due to the discharge of load from the structure, structural elements may redistribute a parcel of the load to another element. This means that, structure and foundation cannot be taken into account separately, they are interdependent and need to be analyzed together.

5 Estimating pile capacity

As mentioned in Section 2.2, it is important to understand the basic principles and practices of the other fields, therefore, this chapter will be concentrated on explaining the theories and ways that piles can be analyzed. The aim of this chapter is to introduce concepts and rise understanding of general theories of pile analysis.

Let us start by saying that, although the lateral resistance of piles implies in calculating the maximum lateral pressure of the soil [11], which is the common idea of pile resistance calculations, one cannot correctly estimate the soil resistance without considering the movements and deformation of the soil-foundation system as the resistance and deflection are interdependent and must be calculated together [8], [22]. Worth mentioning as well is that the analysis of laterally loaded pile is a soil-foundation interaction process that requires careful and continuous considerations from both geotechnical and structural sides [8].

5.1 General pile behavior and limiting pressure

To better exemplify the fundamentals of a pile behavior, let us consider a pile statically loaded in the horizontal direction, the load applied on the pile will increase compression stresses in the soil in front of it and decrease the stresses behind it. As a consequence, soil will be compressed and will move away from the pile in front of it and towards the pile behind it, as exemplified in Figure 14 (a). At some loading stage the soil next to the surface in front of the pile will fail as a wedge mechanism and a gap will appear behind the pile (Figure 14 (b)) [11]. This failure mechanism should be avoided by calculating a limiting pressure for the soil, which depends on the failure mode of the pile.

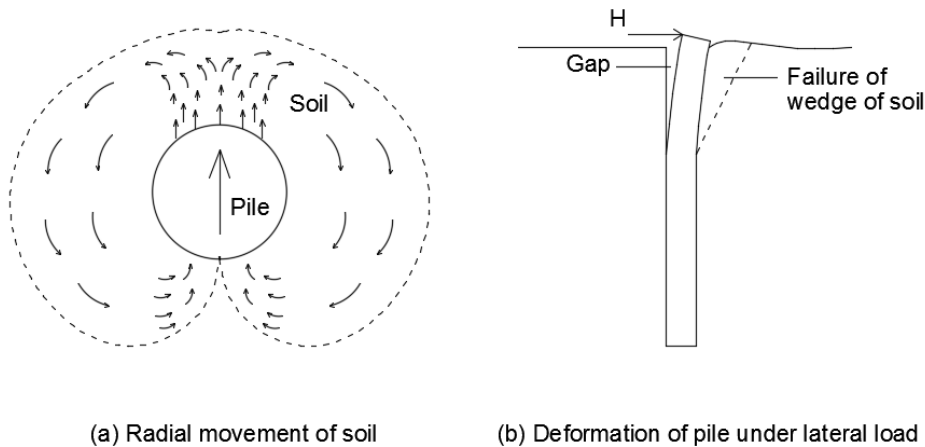


Figure 14: Soil-pile failure behavior (adapted from [11]).

Let us now divide piles into two groups: short and long piles. Short piles (or rigid

piles) rotate around a point at some depth in the soil, this behavior is due to the fact that the pile has not enough anchorage in the toe to avoid full rotation. Above the rotation point, soil pressure will be developed in front of the pile, while bellow the center of rotation, soil pressure will be developed behind the pile, as shown in Figure 15 (a). The failure of this mode is controlled mainly by the soil. A long pile restrains this rotation and a plastic hinge will be developed at certain depth in the soil. Soil pressure will be developed over and bellow the hinge point, as demonstrated in Figure 15 (b), however, only the part above the hinge will undergo considerable displacement and it is the part of interest for calculating the resistance. This failure mode is mainly controlled by the the resistance of the foundation to flexural solicitation, until the plastic hinge is created. [8], [11], [36]

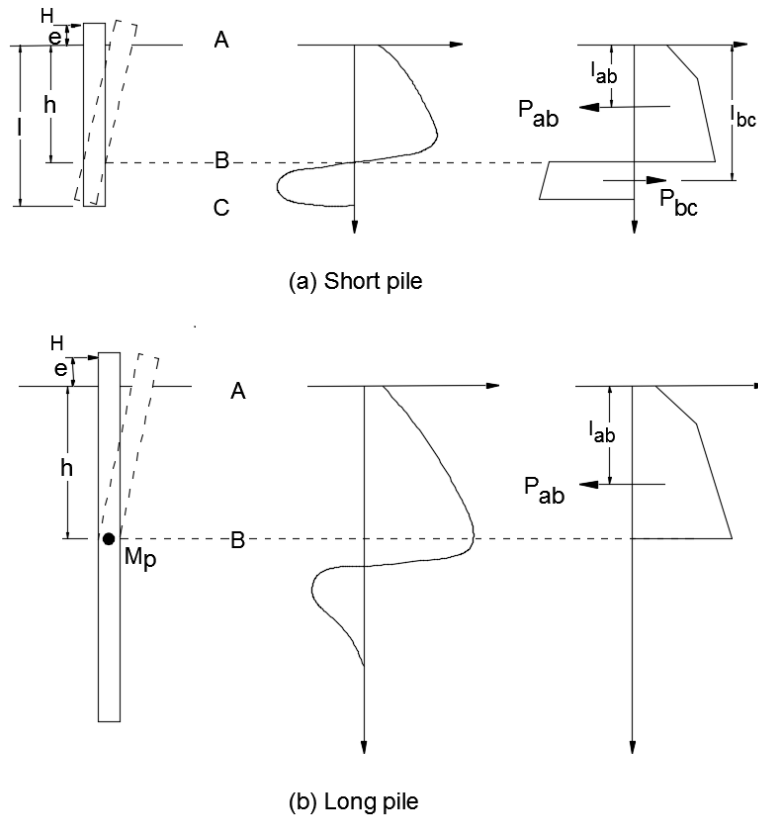


Figure 15: Variation of soil resistance along laterally loaded piles [11].

Considering now a pile cap which restrains the piles from rotation, the failure modes are divided into 3. Short piles with high stiffness, as represented in Figure 16 (a), will translate horizontally as a rigid body and as the pile length and flexibility increases, a plastic hinge will be developed at the connection with the pile cap (Figure 16 (b)), and the pile will start to rotate around a point under the soil. A second hinge can be developed at some depth in the soil for long and slender piles (Figure 16 (c)).

Soil resistance is normally considered as a rigid plastic material, as shown in Figure

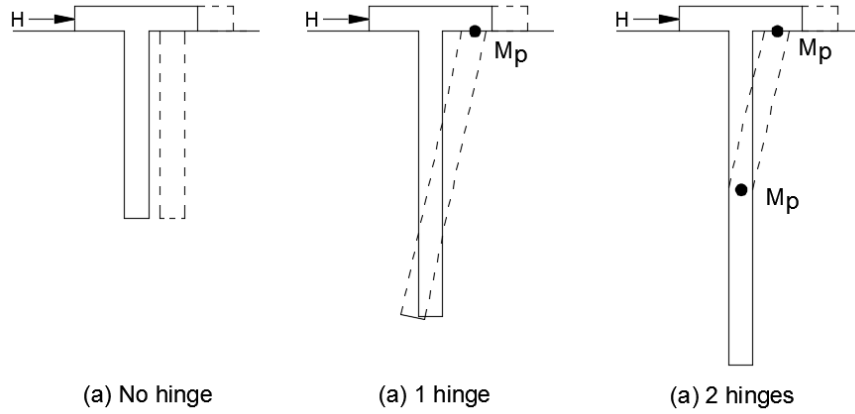


Figure 16: Failure modes for laterally loaded piles [11].

15. For short piles, the moment around the point B is given by the equation (4) and needs to be smaller than the plastic moment of the pile.

$$M_B = P_{bc}(l_{bc} - h) \quad (4)$$

Where:

- M_B is the applied horizontal force (kN)
- P_{bc} is the resultant of the compression force in the soil from point B to C (kN)
- l_{bc} is the distance from the soil surface to the force resultant P_{bc} (m)
- h is the depth from the soil surface to the point B (m)

The horizontal forces equilibrium is:

$$H = P_{ab} - P_{bc} \quad (5)$$

Where:

- H is the moment around point B (kN*m)
- P_{ab} is the resultant of the compression force in the soil from point A to B (kN)

While the moment equilibrium is given by:

$$H(e + h) = P_{ab}(h - l_{ab}) + P_{bc}(l_{bc} - h) \quad (6)$$

Where:

- e is the height from the soil surface to the force application point (m)
- l_{ab} is the distance from the soil surface to the force resultant P_{ab} (m)

For long piles with development of a plastic hinge, the force H must be equal to P_{ab} and the moment around the point B must be equal to the plastic moment M_p . The final equation for the moment equilibrium can be written as:

$$H(e + l_{ab}) = M_p \quad (7)$$

Adding the pile caps, the resistance of the short pile moving laterally consists merely in calculating the total pressure over the soil. For the longer pile with one hing and for the long pile with two hinges, the moments are found by merely adding a term M_p in the right-hand side of the equations (6) and (7) respectively. [11]

5.1.1 Limiting lateral pressure: non-cohesive soils

The lateral resistance of soil is different at each layer considered. Close to the surface, at distances smaller than one diameter, the pile will work as a long retaining wall and the limiting pressure at the failure stage (wedge failure) will be limited by the horizontal pressure resistance of the soil presented in Equation 8. Increasing the depth larger limiting pressures can be developed, and while their calculation has been presented by several different forms by different researchers, for almost all natural existing sands it is possible to utilize an intermediate variation of the expressions, this variation is presented in equation 9. [11]

$$P_{ucs} = K_p \sigma'_v d \quad (8)$$

Where:

- P_{ucs} is the limiting pressure close to the surface
- K_p is the passive earth pressure
- σ'_v is the effective vertical tension of soil
- d is the pile diameter (m)

$$P_m = K_p^2 \sigma'_v d \quad (9)$$

Where:

- P_m is the limiting pressure for a single pile (kN/m)

5.1.2 Limiting lateral pressure: cohesive soils

The horizontal resistance of cohesive soils, accordingly to the plastic failure model, considers that the soil will fail in a plane normal to the pile axis. The calculation takes into account the shear strength of the soil and its friction coefficient in contact with the pile. The results varies from perfect smooth piles (equation 10) to perfect rough piles (Equation 12). [11]

$$P_{us} = 9.14 c_u d \quad (10)$$

Where:

P_{us} Limiting pressure for perfectly smooth piles
 c_u is the shear strength of the soil
 d is the pile diameter (m)

$$P_{ur} = 11.94c_u d \quad (11)$$

Where:

P_{ur} Limiting pressure for perfectly rough piles

5.2 General theory of elasticity for piles

A general and simplified theory of elasticity for piles follows the equation of a beam supported by elastic springs. The differential equation (Equation 12) is valid for an analysis where no axial force is existent, the stiffness EI of the pile is constant and the soil modulus k is constant. [19], [22]

$$EI \frac{d^4 y}{dz^4} - ky = 0 \quad (12)$$

Where:

EI is the stiffness of the pile cross-section
 y is the horizontal deflection
 k is the elastic constant of the soil
 z is the depth under surface.

The solution is found by solving the differential equation and applying the boundary conditions governing the system.

The portion of the pile that would actually transfer lateral load in such conditions could be calculated with the equation 13. This means that the lateral load is transferred along the critical length until it dies out when $z = l_{cr}$, and below it no lateral loads will be left to transfer. [11]

$$l_{cr} = 4 \left(\frac{EI}{k} \right)^{\frac{1}{4}} \quad (13)$$

Where:

l_{cr} is the critical length of the pile

The problems with this method come with the fact that there rarely exists a soil with a constant elastic modulus. [22]

5.3 P-y curve: a non-linear method

A pile can be considered as a beam laying over elastoplastic supports, which can be translated into a simple model of a long element supported by lateral elastoplastic springs in certain intervals [19]. A well known model worth mentioning to solve this problem is the p-y method.

This method was named p - y by its users as its principle is to define a relationship between the lateral resistance of the soil at a certain point with its deflection. Figure 17 (a) and (b) shows the soil reaction in function of the lateral displacement, the cross-section is at a soil depth z and the position (a) shows a uniform distribution of stress when no lateral deflection is present. When a lateral deflection y takes place (position (b)), the stress magnitude increases in front of the pile and normally reduces behind the pile. By integrating the area of stress in position (b) we find a force resultant p in opposite direction of the deflection y with unit force per pile length. For any deflection y and any depth z the resultant value of p will change until reaching the ultimate load. [2], [8], [22]

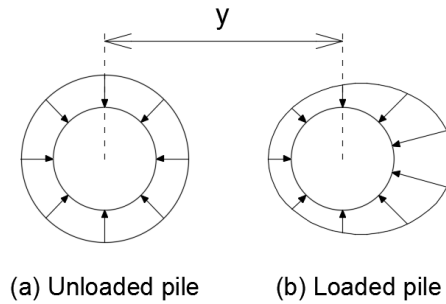


Figure 17: Distribution of stress in a pile cross section at a soil depth z (adapted from [22]).

In practical utilization, due to the availability of software, the method can be viewed as the division of the pile into n segments with stiffness EI connected by nodes; each node is associated to a non-linear spring in which its deformation properties is characterized by the p - y curve of the node, see Figure 18. Boundary conditions are needed, whether the pile head is fixed or free, and by applying load increments and a static equilibrium it is possible to compute the overall deflection of the pile, and its internal forces. [8]

The solution for the p - y method is dependent on many factors; soil type, loading nature and duration and depth below surface are some of the characteristics that may affect the results. However, the influence of each of these factors are not well established and the solution received by the method lays on test results. Full scale lateral load tests have been conducted for several soil types and their results have been correlated to standard soil properties in order to backup the calculation of the p - y curve. For large projects it is sometime recommended that lateral load test are

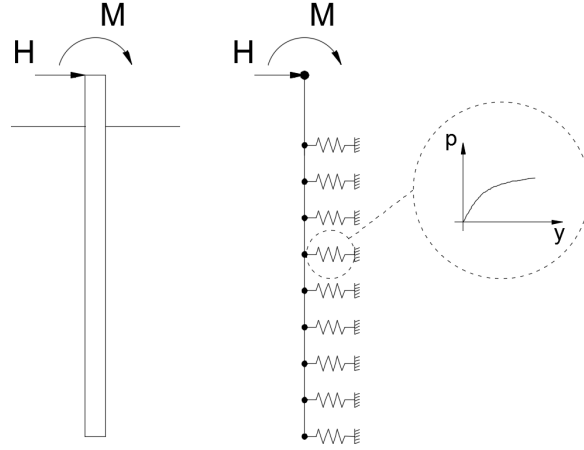


Figure 18: Analytical spring model. Adapted from [8] and [11].

made to develop site specific curves. [2], [8]

Therefore, for each different soil there is a different calculation process for the p-y curve and there are many commercial and free computer programs offer possibilities for such analysis. The methods of calculation of a p-y curve are not part of the scope of this work.

5.4 Subgrade reaction approach

A simplified method for the calculation of the stiffness of the soil-pile interaction, assumes that soil is elastic. The spring constants k , commonly called *coefficient of subgrade reaction*, are calculated as constant linear springs based on the simple theory that the deflection y is linearly connected to the load P (see equation 14).

$$k = \frac{F}{\Delta x} \quad (14)$$

In this section, it will be described a calculation method based on the research made by Rasi-koskinen, 2014 [21] on the Finnish recommendations for laterally loaded pile calculations. All the calculation procedures found in this section are based in her research and references. For more detailed information, see [21].

5.4.1 Non-cohesive soils

Frictional soils are not time dependent and the settlement happens at the time of loading [35]. In case of static load, the subgrade is considered to grow linearly to a depth of $10d$ (where d is the pile diameter) and can be calculated as follow [23].

$$k_s = n_h \cdot \frac{z}{d} \quad (15)$$

Where:

- k_s is the modulus of subgrade reaction (kN/m^3)
- n_h is the constant of horizontal subgrade reaction(kN/m^3)
- z is the depth of soil (m)
- d is the external diameter of the pile

The constant of horizontal subgrade reaction n_h can be extracted in a relation with the friction angle of the soil as presented in RIL 245-2011 [24], or with the equation (16) presented in RIL 212-2001 [23].

$$n_h = \alpha \cdot \beta \cdot \frac{M}{z} \quad (16)$$

Where:

- n_h is the constant of horizontal subgrade reaction(kN/m^3)
- α is 0,74 accordingly to Terzaghi and 1,0 accordingly to Poulos
- β 0,83...0,95 for sand with Poisson ration varying from 0,25 to 0,15 respectively
- M is the compressibility modulus (kN/m^2)
- z is the depth of soil (m)

β can also be calculated with Equation (17). [12]

$$\beta = \frac{(1 + \nu)(1 - 2\nu)}{1 - \nu} \quad (17)$$

Where:

- ν is the Poisson ratio

The compressibility modulus is dependent on the stress deformation levels. Calculated with the Equation (18). [24]

$$M = 100 \cdot m \cdot \left(\frac{\sigma'_v}{100} \right)^{1-\beta} \quad (18)$$

Where:

- M is the compressibility modulus (kN/m^2)
- m is the modulus number accordingly to annex A
- β is the tension exponent accordingly to annex A
- σ'_v is the effective vertical tension (kN/m^3)

5.4.2 Cohesive soils

In fine and cohesive soils one can relate the subgrade reaction with the undrained shear strength of the soil. In normally consolidated soils, the subgrade reaction will increase constantly, where in over consolidated soils the subgrade reaction is nearly constant [21]. Terzaghi (1955) [35], during his lateral loading experiments, discovered that for long term loads the subgrade reaction tends to decrease due to the consolidation of the soil. This concludes that the subgrade reaction is dependent

on the loading time. The two equations bellow can be utilized accordingly to the loading time [24].

For long term loads

$$k_s = 20 \dots 50 \cdot \frac{S_u}{d} \quad (19)$$

For short-term loads

$$k_s = 50 \dots 150 \cdot \frac{S_u}{d} \quad (20)$$

Where:

- k_s is the modulus of subgrade reaction (kN/m^3)
- S_u is the undrained shear strength (kN/m^2)
- d is the external diameter of the pile (m)

5.4.3 FEM spring model for non-cohesive soils

For non-cohesive soils, Figure 19 shows the connection of the maximum pressure allowed P_m with the maximum displacement y_m calculated accordingly to the spring value k_s to a given pile. The dotted line, corresponding to $k_s/2$, connects the maximum points but does not describe the true behavior of the soil.

The calculation can be performed by utilizing the linear spring value k_s , and if the displacement $y > y_m/4$, the substrate reaction needs to be reduce and calculation needs to be performed again. If $P > P_m/2$ and/or $y > y_m/4$, another method of reduction is to apply a load reaction equals to $P_m/3$ and set a new spring equals to $k_s/3$. Calculation should be run again and if $y > y_m$ the load reaction with a value of P_m should be applied to the support. Calculations should be run until any of the terms above is fulfilled. [12], [21]

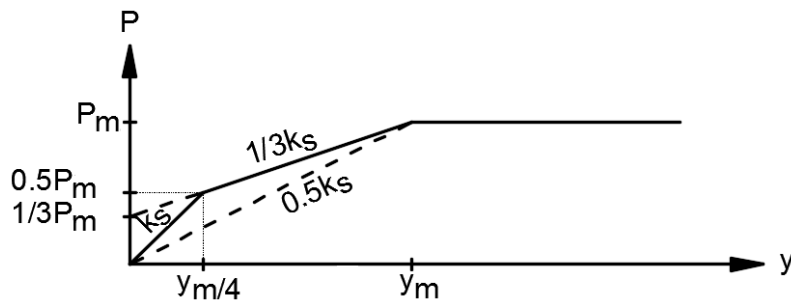


Figure 19: Relation between pile pressure and displacement. Adapted from [24].

5.4.4 FEM spring model for cohesive soils

For cohesive soils, Figure 20 shows the connection of the maximum pressure allowed, P_m , with the maximum displacement, y_m , calculated accordingly to the spring value k_s , to a given pile to both short and long term loading. The dotted lines corresponding to $k_s/3$, for short-term loads, and $0.4k_s$, for long-term loads, connect the maximum points but does not describe the true behavior of the soil.

The calculation can be performed by utilizing the linear spring value k_s , and if the displacement $y > y_m/6$ for short-term loads and $y > y_m/5$ for long-term loads, the substrate reaction needs to be reduce and calculation needs to be performed again. If $P > P_m/2$ and/or $y > y_m/6$ for short-term loads and $y > y_m/5$, another method of reduction is to apply a load reaction equals to $0.4P_m$ for short-term loads and $0.375P_m$ for long-term loads and set a new spring equals to $30S_u/d$ for short-term loads and $12.5S_u/d$ for long-term loads. Calculations should be run again and if $y > y_m$ the load reaction with a value of P_m should be applied to the support. Calculations should be run until any of the terms above is fulfilled. [12], [21]

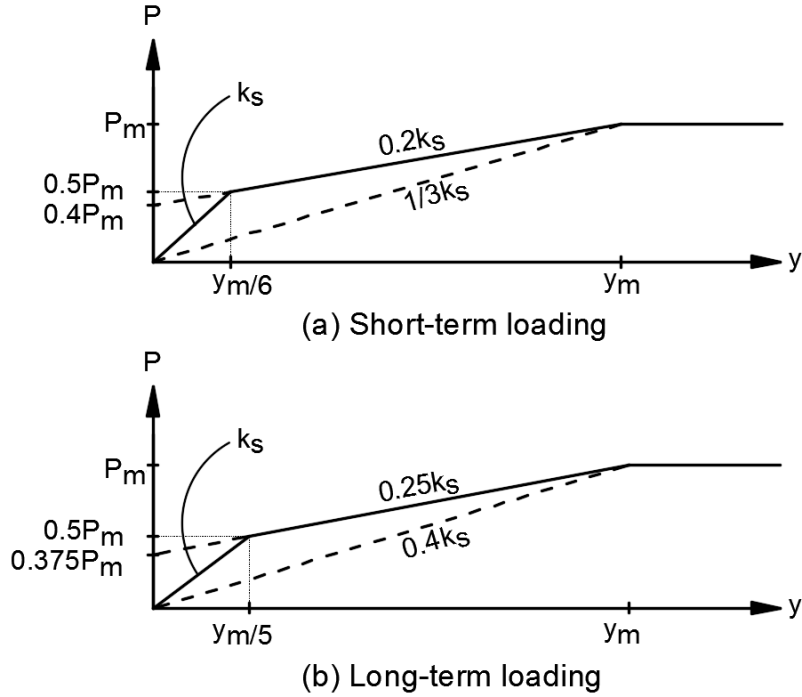


Figure 20: Relation between pile pressure and displacement in cohesive soils. (a) short-term loading, (b) long-term loading. Adapted from [24]

6 Pile groups

It is common that a single pile does not have resistance against lateral loads, so pile groups assembled with a reinforced concrete cap is usually used in foundation engineering [26]. In this chapter, it will be explained the common theories of pile groups effect on behavior of a single pile within the group.

6.1 General pile group theory

Unfortunately, the behavior of laterally loaded pile groups is more complex than that of axial loaded groups and experimental data of pile groups under lateral loads are limited. Therefore, designing pile groups can be a very demanding task when it comes to analyzing the solicitations in each pile of the group, the group deflection, the behavior of the soil-group interaction and the overall resistance of the pile group (group efficiency). [8], [22].

The distance between piles in a group influences the capacity of the piles, meaning that, in certain arrangements the capacity of a pile in the middle of a group is smaller than that of an isolated pile. This is due to the modification of tension when the piles are driven or cast into the soil. If the piles are multiples diameters apart, the group interaction over the soil will not happen and the behavior of the group can be taken as separated piles fully enclosed by soil (see Figure 21 (a)). As piles get closer together, in a simplified theory, it is possible that the soil between piles move together with the piles generating a row or a block failure (see Figure 21 (b) and (c)). The latter block failure will generally happen when the shear resistance of the soil is smaller than the resistance of a single pile, a block failure system of rows of piles (b) will be the most occurring case. The front pile will remain with its full resistance whereas the back pile resistance will be equal to the shear planes resistance between the piles, as expressed in equation 21. A plan overview of this failure system is demonstrated in Figure 22. [11]

$$P_{u, \text{back pile}} = 2\tau_s s \quad (21)$$

Where:

$P_{u, \text{back pile}}$	is the limiting force resistance of a pile behind another pile
τ_s	is the plan shear resistance
s	is the spacing between piles

The description above considers that the soil has the same deflection as the piles enclosing it and could also be treated as an unique pile with a large diameter enclosing the group. However, it might not take into account the true characteristics of the soil. Other approaches are based on reducing the resistance of the whole group, as written by Equation 22, however, the reduction factor is a problem specific of each case and there is no rational method to find a generalized coefficient. [22], [26]

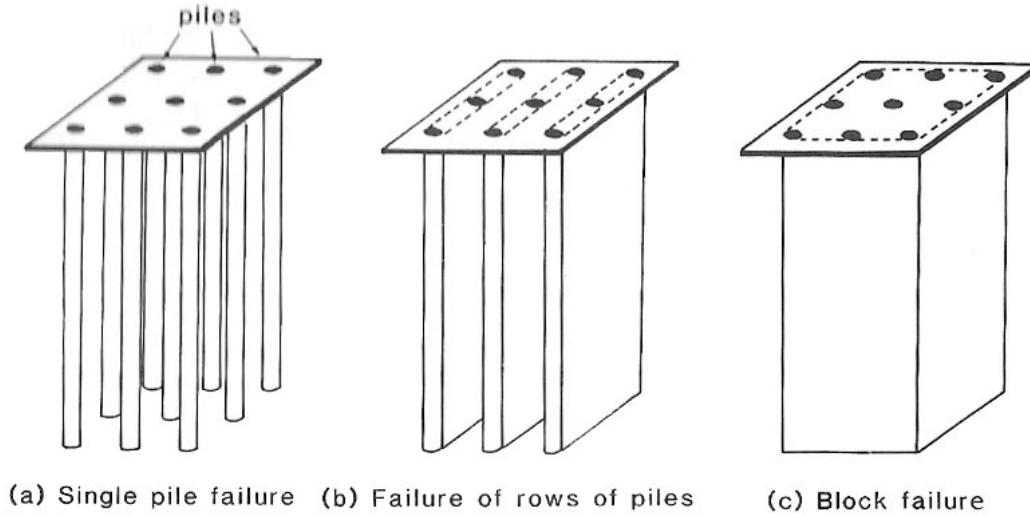


Figure 21: Pile group failure modes [11]

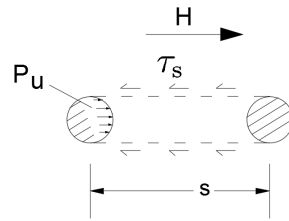


Figure 22: Failure mechanism [11]

$$P_{\text{group}} = e.n.P_{\text{pile}} \quad (22)$$

Where:

- P_{group} is the final group resistance
- e is the reduction coefficient
- n is the number of piles in the group
- P_{pile} is the individual piles resistance

6.2 Introduction to p-multiplier in group interaction

The reality in engineering is that hardly ever the piles will be enough apart to behave as separate piles, and in the most of the cases piles will interact within the group reducing the effectiveness of the group. This was showed by literature and experimental research done by Bowles (1997) [2], Brown et al (1988) [4] and Elhakim et al (2014) [10], where it was proved that a pile group has larger deflection than a single pile when the same loading ratio per pile is kept, meaning that for an hypothetical case of a group of 4 piles with an applied horizontal force of 40kN, the horizontal displacement would be greater than in a single pile with an applied horizontal force

of 10kN. The displacement of the pile group also increases when piles are closely spaced.

Pile-soil-pile interaction is the reason why a pile in the middle of a group has less resistance than a single pile [22]. To take into account this reduction, a p -multiplier f_m was introduced to reduce the portion p , or the p - y curve, of a single pile to create the group-pile curve, as illustrated in Figure 23 [4], [22].

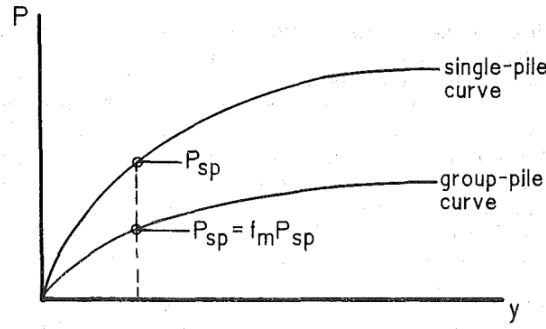


Figure 23: Single pile vs group-pile curve [22]

In a pile group, piles located behind other piles (trailing piles) have less lateral resistance than front rows, in other words, have smaller f_m . This is due to the so called *shadowing effect* (see Figure 24), additionally, edge effects starts to be developed in higher deflections contributing to the reduction of the resistance of the pile [29]. Figure 24 also presents gaps that are left by the deformation of a pile in front of a row and relieves part of the stress in the soil behind it, which in its turn also provides less resistance for the trailing pile [22].

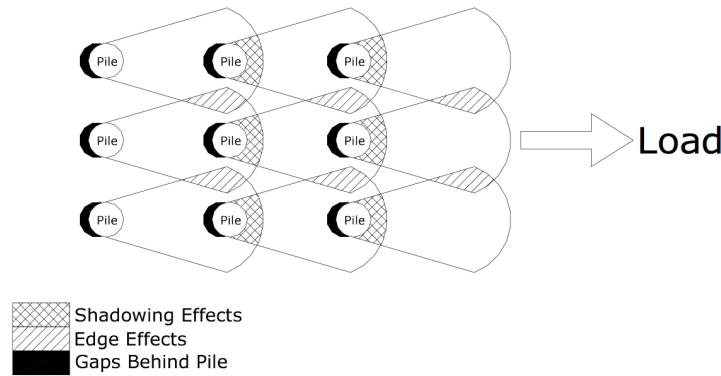


Figure 24: Shadow and edge effect illustrated by Snyder (2004) [29]

6.3 Experimental researches on the p -multipliers

Brown et al (1987) [3] conducted a large scale experiment concerning the behavior of closely spaced piles in a 9-pile group on stiff preconsolidated clay. The pile group had

a 3-by-3 distribution pattern spaced of 3 diameters from center to center of piles and subjected to a two-way cyclic loading. His results show that trailing piles have greater resistance in small deflections and even reduced resistances as deflection increases, whereas front piles seems to have a constant efficiency. He also concludes that a key element to predict the behavior of a pile group is to understand the ultimate lateral resistance in the group. However, there exists no useful and verified theoretical method to predict such resistances under certain circumstances. P-multipliers on the experimental data collected by Brown et al (1987) [3] were later reported by Brown and Shie (1991) [5]. These factors are shown in Table 1.

Table 1: P-multipliers reported by Brown and shie (1991) on data collected by Brown et al (1987)

Row position	30 mm deflection	50 mm deflection
Lead row	0.70	0.70
Second row	0.60	0.50
Third row	0.50	0.40

Brown et al (1988) [4] conducted a similar large scale test as Brown et al (1987) [3]. The pile group was the same but a top layer of stiff clay was replaced by medium dense sand. The results showed that the pile response was closely related to the position of the pile and front piles had larger resistance followed by middle piles and back piles with the smallest resistance. Moreover, by analyzing the data from 1 and 100 loading cycles he mentions that, leading piles showed an efficiency factor near 1, middle piles showed a reduction of 0.4 and 0.35 and back (trailing) piles showed a reduction of 0.3 and 0.25 for 1 and 100 loading cycles respectively.

McVay et al (1998) [13] performed a test in loose and medium dense sand with pile groups varying from 3 to 7 rows and a space of 3 diameters from center to center. Based on the data collected and comparing with previous authors he suggested p-multipliers as shown in Table 2. In his conclusion he confirms the p-multiplier concept put forward by Brown (1988) [4] and states that the sand density did not affect the efficiency of a pile row.

A series of static load test was conducted by Snyder (2004) [29] on a 15-pile group arranged 3-by-5 and spaced 3.92 diameter from center to center. The pile group was enclosed by an upper layer of cohesive soil of soft and medium consistence. Based on test results, he concludes that for group deflections up to 38mm, p-multipliers were 1.0, 0.87, 0.64, 0.81 and 0.70 for rows 1 to 5 respectively, and for larger deflections the multipliers were 1.0, 0.81, 0.59, 0.71 and 0.59.

Walsh (2005) [38] utilized the same pile group tested by Snyder (2004) [29] and changed the layers of cohesive soil by washed concrete sand. Cyclic static loads from 1 to 10 cycles were analyzed and p-multipliers were back calculated, as shown in Table 3. He explains that the results obtained in the tenth cycle are more limited

Table 2: Suggested p-Multiplier for laterally loaded piles by McVay et al (1998) [13]

Row position (1)	Three rows (2)	four rows (3)	Five rows (4)	Six rows (4)	Seven rows (6)
Lead row	0.8	0.8	0.8	0.8	0.8
Second row	0.4	0.4	0.4	0.4	0.4
Third row	0.3	0.3	0.3	0.3	0.3
Forth row	-	0.3	0.2	0.2	0.2
Fifth row	-	-	0.3	0.2	0.2
Sixth row	-	-	-	0.3	0.2
Seventh row	-	-	-	-	0.3

than those obtained in the first cycle due to limitations in the target deflection, this suggests that p-multipliers obtained in the first cycle are more applicable to a wider range of deflections. Finally, the author suggests that soil strength should be reduced for loading with 10 or more cycles.

Table 3: Suggested p-Multiplier by Walsh (2005) [38]

	p-multiplier	
Row	Cycle 1	Cycle 10
Row 1	1	1
Row 2	0.5	0.6
Row 3	0.35	0.4
Row 4	0.3	0.37
Row 5	0.4	0.4

6.4 Implementation of equation for modified pile spacing

Some works were done trying to implement general equations in order to take into account the pile-soil-pile interaction in pile groups making use of experimental tests such as the ones mentioned in the previous section. Some of these works are described in this section.

6.4.1 Pile efficiency factor for pile groups by Reese (2006) [22]

Reese et al (2006) [22], based on the work of Brown et al. (1987) [3], presents a suggestion for calculating p-multipliers f_m . His proposal makes use of other works, technical literature, and results of pile group tests performed by other authors. The calculation of the p-multiplier is for individual piles instead of an entire row of pile, however it does not take into account the soil type. The calculation procedure is

described as follow

Reduction of side-by-side piles

The first reduction to be considered is the side-by-side pattern, which is the distribution of piles in the perpendicular direction of the force (the curve and the schematics can also be seen in Annex C). The reduction can be calculated the Equation 23.

$$e_{\text{side}} = 0.64 \left(\frac{s}{b} \right)^{0.34} \text{ for } 1 \leq \frac{s}{b} < 3.75; \quad \text{otherwise : } e_{\text{side}} = 1 \quad (23)$$

Where:

- e_{side} is the reduction factor
- s is the spacing of piles to their center
- b is the pile diameter

Reduction of line-by-line piles

Another pattern in the reduction is the lines of piles (can also be found in Annex C). In this case, the reduction of the leading piles is smaller than that of a trailing pile (pile that is found behind of the leading pile, as represented in Figure 25). Equation 24 gives the reduction for the leading piles while Equation 25 gives the reduction for a trailing pile.

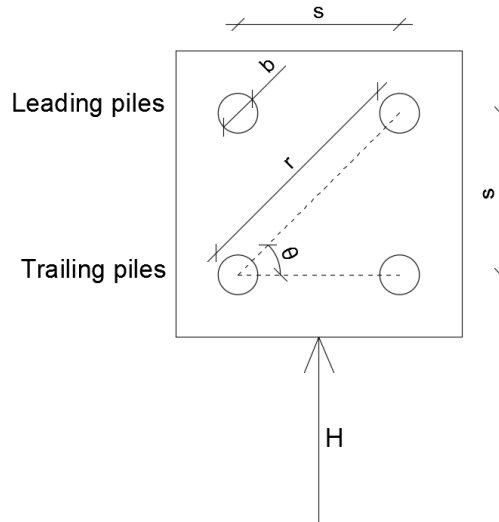


Figure 25: Leading, trailing and skewed piles

$$e_{\text{leading}} = 0.70 \left(\frac{s}{b} \right)^{0.26} \text{ for } 1 \leq \frac{s}{b} < 4.0; \quad \text{otherwise : } e_{\text{leading}} = 1 \quad (24)$$

$$e_{\text{trailing}} = 0.48 \left(\frac{s}{b} \right)^{0.38} \quad \text{for } 1 \leq \frac{s}{b} < 7.0; \quad \text{otherwise : } e_{\text{trailing}} = 1 \quad (25)$$

Reduction of skewed piles

Reduction effects also need to be taken into account in the diagonal direction, which are named as skewed piles. These piles are demonstrated in Figure 25 by the two piles located in the corners, separated by a distance r , and with an angle θ from the horizontal direction. The reduction can be calculated by utilizing Equation 26 where the side-by-side coefficient e and the line-by-line coefficient e_{line} are calculated by utilizing the relation $\frac{r}{b}$ in place of $\frac{s}{b}$, where r can be seen in Figure 25, and the reduction coefficient e_{line} can be either from leading pile or trailing pile depending whether we are analyzing the piles in the front or back row.

$$e_{\text{skewed}} = (e_{\text{line}}^2 \cos^2 \theta + e_{\text{side}}^2 \sin^2 \theta)^{\frac{1}{2}} \quad (26)$$

Assembling the coefficients together

As an example of the reduction coefficient, let us take the right upper and lower piles shown in Figure 25, the total reduction factor of the upper corner pile would be the multiplication of the side-by-side, line-by-line leading and skewed factor, with the last factor calculated with e_{leading} in place of e_{line} by utilizing the relation $\frac{r}{b}$ in place of $\frac{s}{b}$. Whereas the total reduction factor of the lower corner pile would be the multiplication of the side-by-side, line-by-line trailing factor and skewed factor, with the last factor calculated with e_{trailing} in place of e_{line} by utilizing the relation $\frac{r}{b}$ in place of $\frac{s}{b}$.

6.4.2 Pile row efficiency factor by Rollins et al (2006) [25]

Rollins et al (2006) [25] back-calculated p-multipliers using the results of 3 large scale lateral load tests on pile group up to 5 rows in stiff clay. The piles varied the center to center spacing from 3.3 to 5.65 pile diameters. It was then suggested 3 equations to take estimated the behavior of leading and trailing rows, as shown below. Rollins et al (2006) applied the suggested p-multipliers in two software for pile group analysis and concluded that the results obtained correlated very well with the full scale test.

Front row:

$$f_m = 0.26 \ln \left(\frac{s}{b} \right) + 0.5 \leq 1 \quad (27)$$

Second row

$$f_m = 0.52 \ln \left(\frac{s}{b} \right) + 0.5 \leq 1 \quad (28)$$

Third or higher rows

$$f_m = 0.60 \ln \left(\frac{s}{b} \right) - 0.25 \leq 1 \quad (29)$$

6.4.3 Pile row efficiency factor by Al-Shamary et al (2018) [1]

In order to cover the lack of comparative researches between cohesive and non-cohesive soils, Al-shamary et al. (20018) utilized a three-dimensional finite element approach with varied group geometries (2-by-1, 2-by-2 and 3-by-2) and four pile spacing (2, 4, 6 and 8 diameters). The p-y curves obtained in both cohesive and non-cohesive soils made it possible to develop an equation in function of pile spacing s and pile diameter b to estimate a p-multiplier. The proposed solution, Equation 30, makes use of two coefficients (A and B) which can be directly obtained from Table 4.

$$f_m = A \ln \left(\frac{s}{b} \right) + B \leq 1 \quad (30)$$

Table 4: Values of A and B for non-cohesive and cohesive soils [1]

Group configurations	Trailing row		2nd Trailing row		Leading row	
	A	B	A	B	A	B
Non-cohesive soil						
2 x 1	0.2031	0.2806	-	-	0.1154	0.5686
2 x 2	0.2075	0.2575	-	-	0.1867	0.4018
3 x 2	0.2272	0.1445	0.2014	0.2403	0.1612	0.4052
Cohesive soil						
2 x 1	0.2234	0.1870	-	-	0.2356	0.2955
2 x 2	0.1973	0.1852	-	-	0.2292	0.2890
3 x 2	0.2304	0.0543	0.1246	0.2578	0.2092	0.2718

Furthermore, Al-Shamary et al. (2018) [1] carried out a research on 13 authors (among them Brown and Shie (1991) [5], Brown et al. (1987) [3], Brown et al. (1988) [4], McVay et al. (1998) [13] and Rollins (2006) [25]) and compared the results with the predicted p-multipliers calculated by Equation 30, which had a general good agreement with the experimental results. An average equation was also proposed by Al-Shamary et al. (2018), which was based on the average values between the experimental and the computational results (see Equation 31). The conclusion was that both equations show good agreement to trailing rows but lower values to leading rows when comparing to experimental results.

$$f_{m(\text{average})} = A' \ln \left(\frac{s}{b} \right) + B' \leq 1 \quad (31)$$

Table 5: Values of A' and B' for both non-cohesive and cohesive soils [1]

Group configurations	Trailin row		2nd Trailing row		Leading row	
	A'	B'	A'	B'	A'	B'
2 x 1	0.1042	0.2032	-	-	0.0519	0.5879
2 x 2	0.0779	0.2107	-	-	0.0581	0.4920
3 x 2	0.1071	0.1136	0.1179	0.1264	0.0304	0.6214

6.5 Summary of results

A summary of the data collected and exposed in the previous section was carried out in order to better visualized the p-multipliers suggested by each author. Two tables were constructed, Table 6 contains the results for non-cohesive soils and Table 7 contains the results for cohesive soils.

P-multipliers were also calculated with the suggested equations developed by Reese et al. (2006), Rollins et al. (2006) and Al-Shamary et al. (2018) with the same pile spacing used in the experimental data (3 and 3.92 pile diameters). The calculations of the method proposed by Reese et al. (2006) was applied on a pile group distribution of 3-by-3 and was the most extensive one to calculate, the assembling of data is presented in Annex C. Calculations with the equations proposed by Rollins et al. (2006) were only compared to cohesive soils, since the pile group test was performed on over consolidated stiff clay. Calculations with the equations proposed by Al-Shamary (2018) were carried out for both cohesive and non-cohesive soils and the geometry utilized for the coefficients A and B were those of 2-by-3 pile group.

It is observed that the p-multiplier for the first row calculated with the equation proposed by Al-Shamary et al. (2018) and p-multipliers for the second and third rows calculated with the equation suggested by Reese et al. (2006) are relatively off the average values from the other results in non-cohesive soils (see Table 6). Whereas for cohesive soils (see Table 7), only the coefficient calculated for the first row with the equation proposed by Al-Shamary et al. (2018) and the coefficient for the third row calculated with the equation suggested by Reese et al. (2006) are off the average pattern from other results. The smaller p-multipliers obtained by Al-Shamary et al. (2018) for the first row can be used as a conservative design, while those of Reese et al. (2006) are of higher values and should not be used without proper analysis.

For practical uses, where pile spacing is not equivalent to those presented in this table, it might be of good reason to use equations proposed by Reese et al. (2006)

Table 6: Summary of results up to 5 rows of piles in non-cohesive soils

Author	Sand type	s/b *	Comment	p-multiplier				
				Row 01	Row 02	Row 03	Row 04	Row 05
Brown et al (1988)	Medium dense over stiff clay	3	-	0.8 - 1.0	0.4	0.35	-	-
McVay et al (1998)	Loose and medium dense	3	-	0.8	0.4	0.3	0.2	0.3
Reese et al (2006)	No classification	3	*1	0.86	0.59	0.63	-	-
Al-Shamary et al (2018)	No classification	3		0.58	0.46	0.39	-	-
Walsh (2005)	Clean	3.92	-	1.0	0.5	0.35	0.3	0.4
Reese et al (2006)	No classification	3.92	*1	0.99	0.78	0.78	-	-
Al-Shamary et al (2018)	No classification	3.92		0.62	0.51	0.45	-	-

* s/b is the pile spacing from center to center divided by the diameter of the pile

*1) p-multipliers calculated accordingly to suggested by Reese et al (2006)

to calculate the effect on the first row and to use the equations proposed by Al-Shamary et al. (2018) to estimate the effects on the second and forth row. It is worth mentioning as well that these estimations cannot substitute pile group load tests but are estimations that can be used when pile group tests are not available.

Table 7: Summary of results up to 5 rows of piles in cohesive soils

Author	Soil type	s/b *	Comment	p-multiplier				
				Row 01	Row 02	Row 03	Row 04	Row 05
Brown et al (1987) (*1)	Stiff clay	3	$y^*=30\text{mm}$	0.70	0.60	0.50	-	-
		3	$y^*=50\text{mm}$	0.70	0.50	0.40	-	-
Reese et al (2006)	No classification	3	*2	0.86	0.59	0.63	-	-
Rollins et al (2006)	Over consolidated stiff clay	3		0.78	0.57	0.41	-	-
Al-Shamary et al (2018)	cohesive soil	3		0.50	0.39	0.31	-	-
Snyder (2004)	Soft and medium soil	3.92	$y^* \leq 38\text{mm}$	1.00	0.87	0.34	0.81	0.70
		3.92	$y^* > 38\text{mm}$	1.00	0.81	0.59	0.71	0.59
Reese et al (2006)	No classification	3.92	*2	0.99	0.78	0.78	-	-
Rollins et al (2006)	Over consolidated stiff clay	3.92		0.85	0.71	0.57	-	-
Al-Shamary et al (2018)	cohesive soil	3.92		0.56	0.43	0.37	-	-

*s/b is the pile spacing from center to center divided by the diameter of the pile

*y is lateral deflection of pile group

*1) p-multipliers reported by Brown and Shie (1991)

*2) p-multipliers calculated accordingly to suggested by Reese et al (2006)

7 Methodology of the analysis

This section will bring the steps carried out on this work from the first predictions to the final model. It will also contain the foundation stiffness models chosen and their respective descriptions.

The values sought on these analyses were the variation of the global deformation of the building, which were measured by the top floor maximum displacement, the variation on pile loading distribution and the variation on the distribution of forces in the stiffening system, which were measured by the highest variation of loads in each pile and the shear values of the shear walls in the basement.

7.1 Structural model and considerations

The structural model used was an office building consisting of 23 stories. The first two floors are designated as parking lot and 21 floors as office spaces with the last two floors modified with a terrace. The cross-sections along the building can be seen in Annex D. The structure is cast-in-situ reinforced concrete with its main stiffening system composed of shear walls. All shear walls are 300 mm thick, beams vary from 400 mm x 600 mm to 600 mm x 1000 mm and columns are 600 mm x 600 mm in all office floors and 800 mm x 800 mm in the first two floors. Concrete class in walls and beams is C40/50, columns is C60/75, pile caps is C45/55 and the piles are C50/60 or C45/55 depending on the pile geometry.

The top level of the foundation is 1 meter under the surface of soil and the piles are considered to be pinned at the pile cap and pinned on bedrock, which was considered to be 10 meters deep from the surface of the soil. Foundation blocks are 1.5 to 2 meters thick, therefore, the average depth of the pile head is 3 meters under the soil surface.

A 3D Finite Element model of the building was made in Dlubal RFEM v5.14 ©. Views from the model can be seen in Figure 26. Only the main load bearing structural frame was modeled. Connection between beams and columns are pinned, no bending moment is transferred. Shear walls are all rigid connected.

7.1.1 Vertical loadings

The live loads applied over the structure were under "Category B: office areas" of EN 1990 [31] and chosen of a magnitude of 2.5kN/m^2 accordingly to EN 1991-1-1 [32] Table 6.2. An additional live load of 0.5kN/m^2 was applied to cover lightweight walls and installations. An additional dead load of 0.5kN/m^2 was applied over the solid slabs to model the finishings. Snow loads were applied on the roof according to EN 1991-1-3 [33].

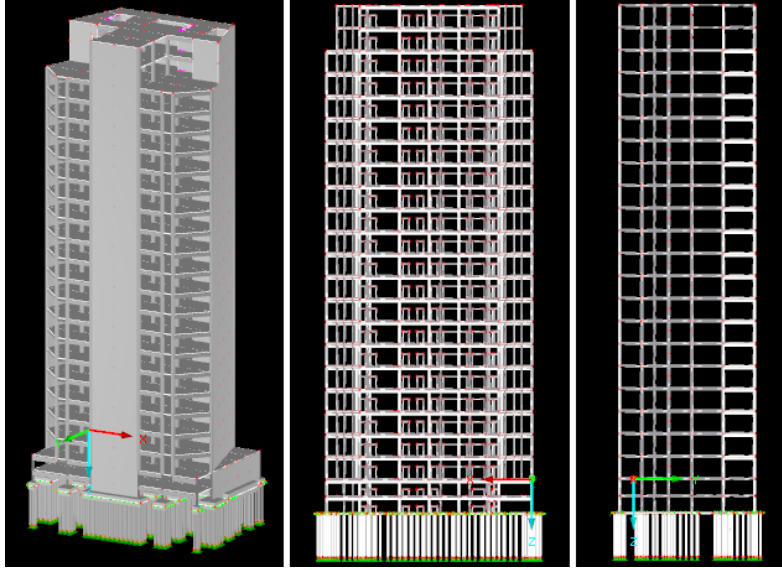


Figure 26: Finite Element Model

7.1.2 Wind loading

Wind forces were calculated accordingly to EN 1991-1-4 [34] for both global positive and negative 'x' and 'y' directions of the structure. Calculation results can be viewed in Annex E.

7.1.3 Loading combinations and analysis type

Ultimate limit state (ULS) and serviceability limit state (SLS) load combinations were set in the models with consideration to Eurocode specifications. A load result combination was created by the combining all ULS load combinations so that extreme values could be easily checked within all loading combinations. ULS load combinations and the result combinations were used to analyze vertical pile loads and shear values on the shear walls. The building deformation was analyzed by using SLS load combinations due to the fact that deformations are part of serviceability state design. Lateral loads of the soil-foundation interaction was also checked with SLS combinations because soil deformation is dependent on the loading it receives and if analyzed with ULS combinations loads would be of higher magnitude, which would mean that soil would deform more than in practice.

Analysis was set in RFEM second-order analysis (P-delta).

7.2 Defining pile distribution and pile group geometry

Pile distribution was primarily based on capacity needed against vertical loads. Bending moment capacity was not considered during pile placement.

To reach a final pile distribution, a process was utilized and the steps were as follows: a preliminary pile distribution was at first based on calculations with simple translation restrained supports (see Figure 27) and their position have been changed until the most optimal reaction distribution was achieved. The limit for vertical reaction was based on the pile capacities presented in Table 8. The pile capacities presented here were taken from the product sheet made available by the Finnish construction industry (see [27]).

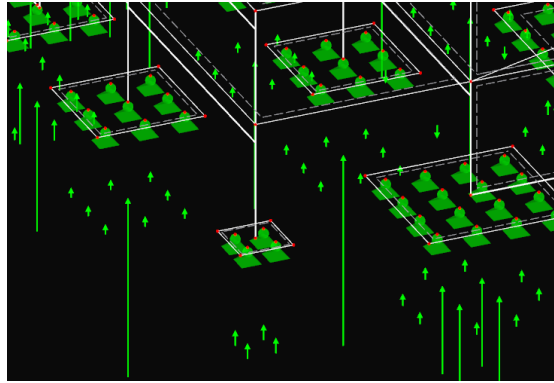


Figure 27: preliminary support distribution: simple supports

Table 8: Pile types and capacities

Pile type	Concrete class (MPa)	Capacity kN		
		PTL3	PTL2	PTL1
TB250a	45	605	544	495
TB250b	45	682	614	558
TB300a	45	870	783	711
TB300b	45	972	874	795
TB300c	50	1124	1012	920
TB350a	50	1509	1358	1234

In a later stage, supports placed directly under upper load bearing elements were subjected to very large loads. It was concluded that it was due to the fact that no deformation was taking place and the foundation was not distributing the load to neighbor supports. Therefore, the simple supports were updated with an elastic constant in the z direction to allow deformation (see Figure 28). The elastic constant was calculated allowing the maximum vertical load in the model to deform 2 mm. This value has no theoretical meaning, it was just implemented so that this would allow displacement and make it possible to achieve a more appropriate load distribution.

Having now a more even vertical load distribution over the supports, the last stage was then to transform the supports into piles, which now had its real vertical stiffness with

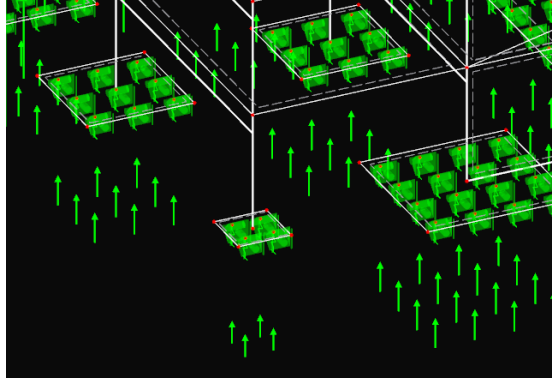


Figure 28: preliminary support distribution: vertical elastic supports

real displacements, which created a new loading distribution. Piles were then finally rearranged in order to even the loads out and reach a better loading distribution. The final pile distribution can be seen in Annex F. Piles were set with the goal to have not more than 80% of average utilization to follow the engineering practices. The model was now ready to receive the implementation of the lateral foundation stiffness models.

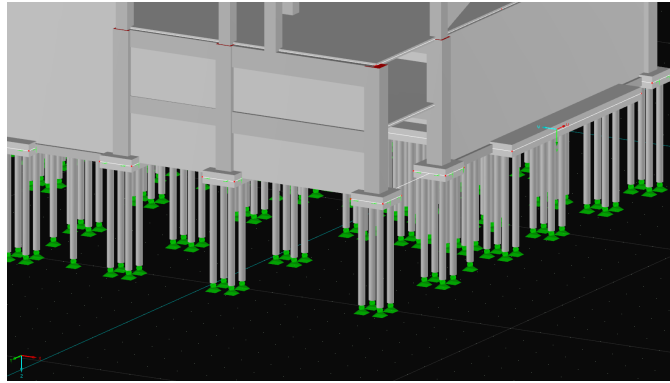


Figure 29: preliminary pile distribution: simple supports

7.3 Soil type and soil-pile analysis

7.3.1 Soil type

The soil type utilized was chosen from the table in Annex A. And as the goal of this work is not focused on soil analysis but how the soil-foundation stiffness modeling affects the structure, the criteria was to use a soil that could easily be analyzed both by the subgrade reaction approach and the p-y curve method. Therefore, it was chosen loose sand $d_{10} > 0.06$, with dry density $\rho = 10kN/m^3$ and friction angle ϕ of 32. For the subgrade reaction method, the modulus number ' m ' and tension coefficient ' β ' were taken from the table in Annex A for loose $d_{10} > 0.06$. For

simplification of analysis the soil stratus was considered to be continuous and with no ground water level.

7.3.2 Subgrade reaction approach

A soil analysis was carried out using the subgrade reaction approach as it is the method that can be found in Finnish guideline books. The method of subgrade reaction was calculated accordingly to Section 5.4 of this work and the limiting pressures based on Section 5.1.1. The results can be seen in Table 9 for all pile geometries available in Table 8.

As the methods utilizes pile diameter for the analyzes and the piles used in the model are square, an equivalent pile diameter was calculated by equivalence of area. The final results which are given in $\frac{kN}{m^3}$ were then multiplied by the pile diameter and the space between the springs so that the unit was $\frac{kN}{m}$ and possible to apply in the model. By making these multiplications, the pile diameter did not affect the value of the subgrade reaction. The limiting pressure, in the other hand, is dependent on the pile diameter. The space of lateral springs was chosen as 0.5 meters at the first meter depth and with 1 meter spacing bellow 1 meter depth. The soil stiffness remains constant after a depth of 10d, therefore the stiffness changes from 3 to 7 meters only.

Table 9: Lateral stiffness of soil based subgrade reaction approach

Depth	k_s (kN/m)	Load capacity (kN)		
		TB350	TB300	TB250
3.00	3423.27	63.48	53.70	44.81
3.50	3697.55	74.06	62.65	52.27
4.00	3952.85	84.64	71.60	59.74
5.00	4419.42	105.79	89.51	74.68
6.00	4841.23	126.95	107.41	89.61
7.00	5229.13	148.11	125.31	104.55
8.00 ...	5229.13	148.11	125.31	104.55

7.3.3 P-y method

The p-y soil-pile stiffness curves were calculated with the free software PyPile 0.6.2 developed by *Yong Technology Inc.* ©.

In order to take into account the cyclic nature of the wind, the analysis was set with 100 loading cycles and loading increasing from 10 to 110kN. It was also simulated the refilling of soil on top of the foundation from excavations, this was done by setting the upper layer of soil with reduced density and friction angle. The pile setup for the square pile TB350a and its head deformation can be seen in Figure 30.

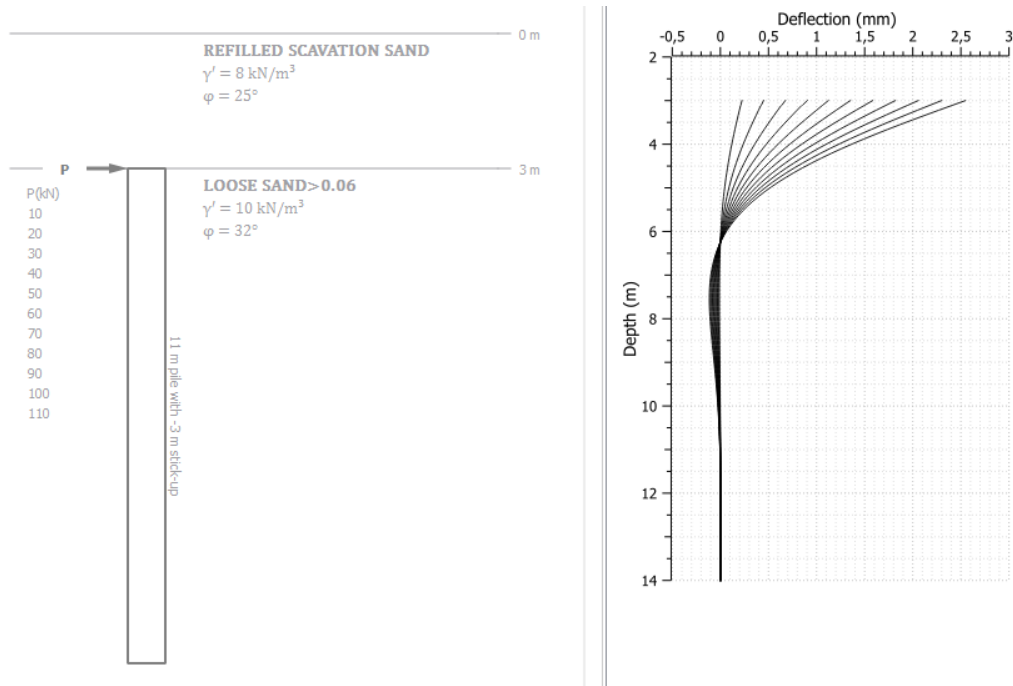


Figure 30: P-y analysis of loose sand

The p-y curves of the setup can be viewed in Figure 31. The division was chosen as in the subgrade reaction approach: 0.5 meters spacing on the first meter and then 1 meter spacing for the layers below. For the analysis in the structural model, it will be intended to stay in small deformations. The reason for that is not to allow large plastic strains to be developed in the soil and stay in the most within a "linear" behavior of the curve.

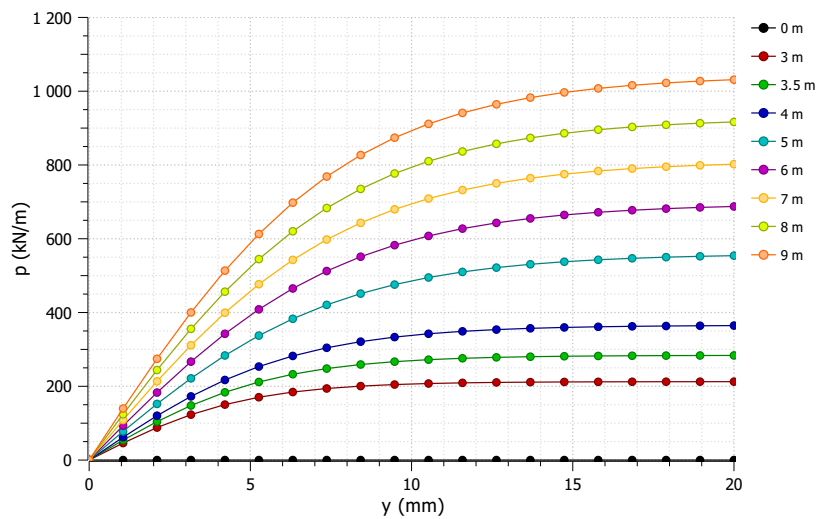


Figure 31: P-y curves of loose sand

7.4 Pile group efficiency

Pile groups were firstly arranged to carry the vertical loads and after that their lateral resistance have been calculated based on the final distribution. The pile spacing used in the model was of 3 diameters from center to center of pile due to the fact that most experimental researches used pile spacing of 3 diameters.

Pile efficiency was chosen by judgment on the average values from the data available in Tables 6 and 7. As the soil used in this work is a soft sand, the values were taken for non-cohesive soils, being 0.90 for the first row, 0.4 for the second row, 0.35 for the third row and 0.20 for the subsequent rows. A pile group effect would look like the example in Figure 32, where the (a) would be the resistance distribution for a loading in the positive x direction, (b) for loading in positive y, and (c) and (d) for negative x and y respectively. A pile groups with group effect in all directions is represented in Figure 32 (e), which each pile has a different set of resistance to each direction. This input into RFEM means 16 different springs for a 4x4 pile group.

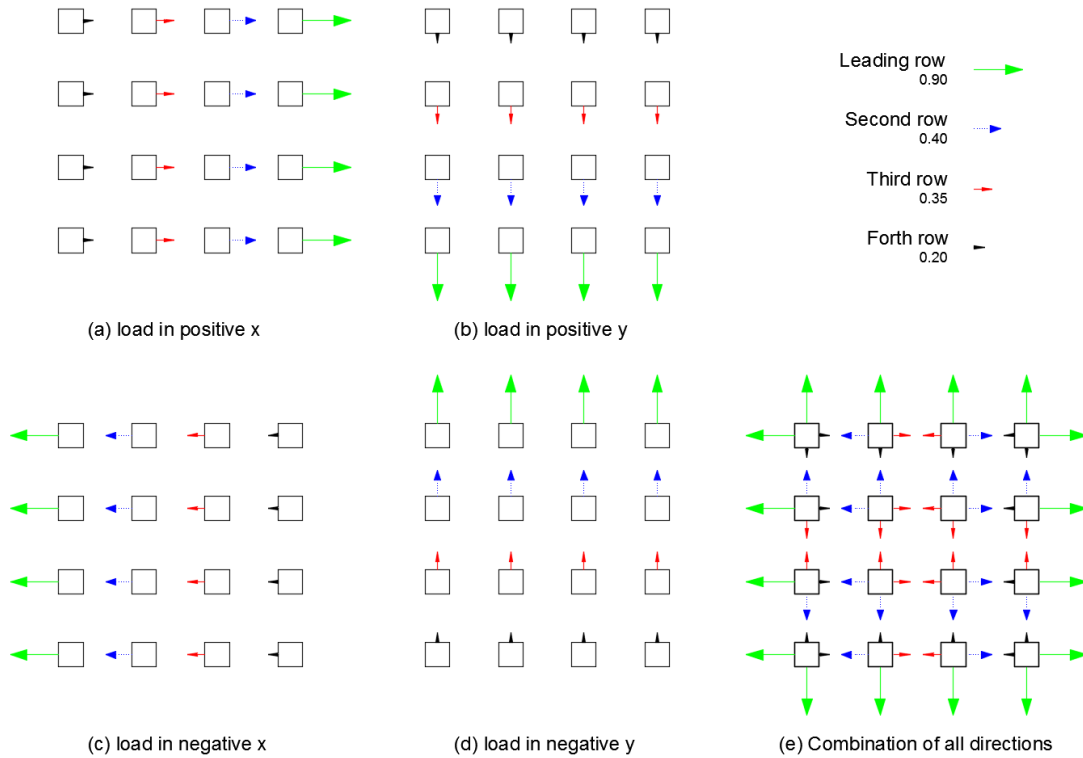


Figure 32: Pile group row efficiency combination

7.5 Soil-foundation stiffness models

The models chosen were set to with two main goals. The first goal was to check the affects of simplification in spring modeling on the structure, and the second goal was to verify what was the magnitude of this affect, therefore, the following models were

proposed and analyzed.

For conservative design intentions, and also to direct this work to practical utilization, only the resistance of the pile shafts were taken into account. The reason of this was already mentioned in Section 4.3: due to probable excavation for the casting of the pile cap and the higher possibility of movement on the pile cap as it is closer to the surface, larger settlements are prone to happen under cyclic loading over time, for this reasons, springs were set only along the pile shaft.

7.5.1 Model 1: Simply supported

After having the pile distribution for the vertical forces, the piles were substituted with simple supports, as shown in Figure 33. This model will be used as a mark for the variation of the following models. This analysis is also important to check the affects of a simple supports on structures, which is similar to what is used in hand calculation checks of building stability.

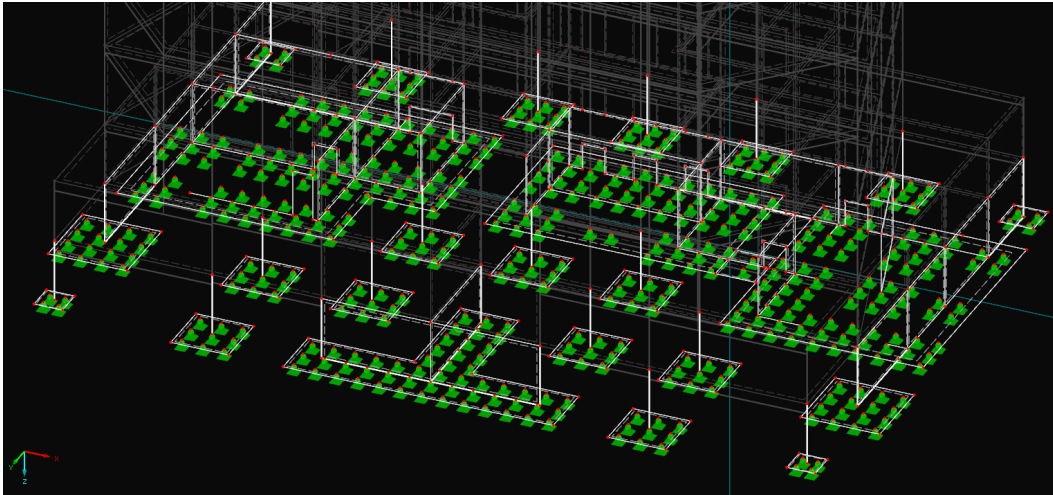


Figure 33: Model 1: Simple supports

7.5.2 Model 2: Subgrade reaction approach with no effects of pile group

Model 2 was set to simulate the typical stiffness model of foundation that may typically be used in Finland. The spring values used in this model were calculated with the subgrade reaction approach and the values can be checked in Table 9 in Section 7.3.2. The maximum capacity of each pile was then calculated using RFEM by applying a load in the pile head until the first spring reached its limiting pressure (see Figure 34), then dividing the force value by the corresponding displacement to estimate a spring constant k'_s for the pile, which would be the slope of the ultimate load capacity of the pile. This procedure took into account the recommendations of Section 5.4.3 (FEM spring model for non-cohesive soils). It is worth mentioning that the procedure mentioned above may not be the current practices of geoengineering

offices, still, it was used in this work to give an estimation of the pile capacity.

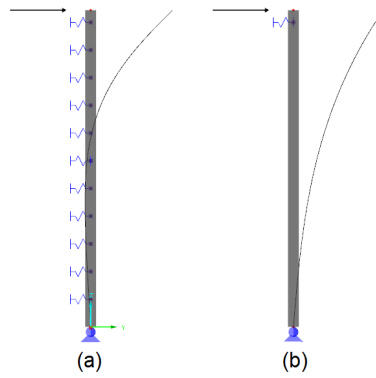


Figure 34: Standard pile models

For the distribution of springs in the model, as it is typical to consider only the resistance of the leading piles in a pile group and then model the spring in the middle of the group, for instance, in Figure 35 this would mean the resistance of the 3 leading piles. Group effects were not considered and springs were modeled in the middle of pile groups chosen as maximum of 3x3 pile groups, as shown in Figure 36

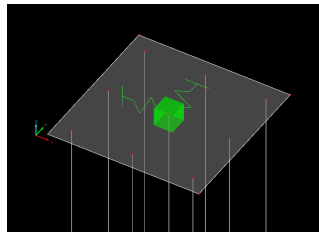


Figure 35: Typical spring distribution

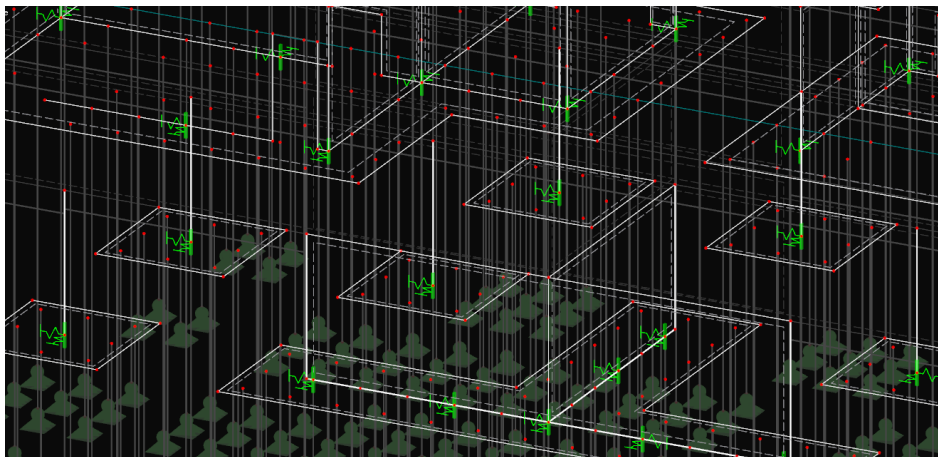


Figure 36: Model 2

7.5.3 Model 3: Based on p-y analysis with 100 cycles

The third model was constructed with springs distributed along the pile shaft at certain depth intervals (Figure 37) and pile group interaction was taken into account. The model looked then like Figure 38.

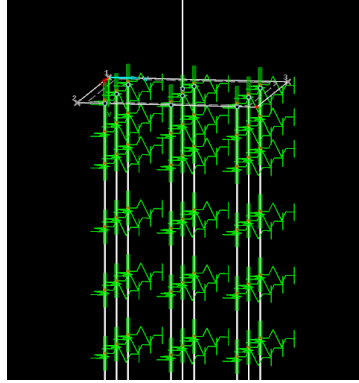


Figure 37: Spring distribution of Model 3

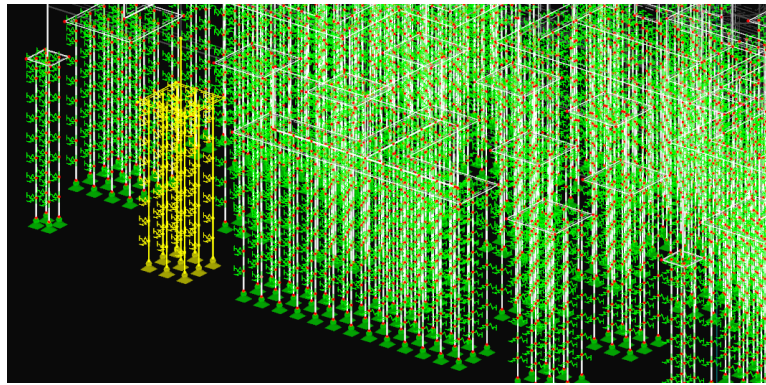


Figure 38: Spring distribution of Model 3

As already mentioned in Section 7.3.3, the deformation was limited to small deflections and the spring coefficients were calculated as demonstrated in Figure 39, which is the most linear part of the p-y curve at 3 meters depth. It is important to mention that when setting springs in such a manner, the model needs to be checked carefully in order to ensure that the deformation of the foundation is not over the limit value of the curve.

To model precisely the group efficiency of large pile groups such as the one shown in Figure 40, the springs could not be set with the same value for each row. Besides the roll efficiency of 0.9 for the first row, 0.40 for the second, 0.35 for the third and 0.20 for the rest of the tailing rows, requires the consideration of the loading direction, as already explained in Section 7.4. To consider this effect in the springs, the following procedure can be adopted: as an example, let us suppose that from the soil analysis

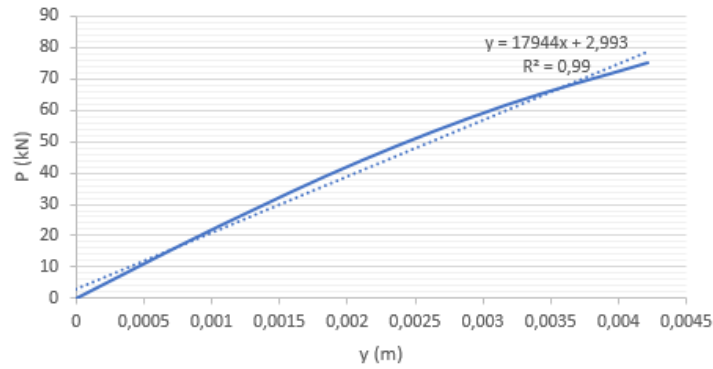


Figure 39: Soil stiffness at 3m

the pile capacity is 10 kN for a 2 mm deflection, the spring model for a pile in the first right row would then have an efficiency of 0.90 if the loading was in positive x direction and 0.20 if the loading was in the negative x direction and the spring modeling could be as shown in Figure 41. However, This would mean having more than 30 different springs for every layer of soil. Only for the pile group in Figure 40 it would be needed more than 240 different springs, reaching almost 2 thousand different springs in the entire model. For that reason, in this model the wind load in the negative direction of x and y was not considered, reducing the model to only 120 different springs for to the wind load in positive x and y directions.

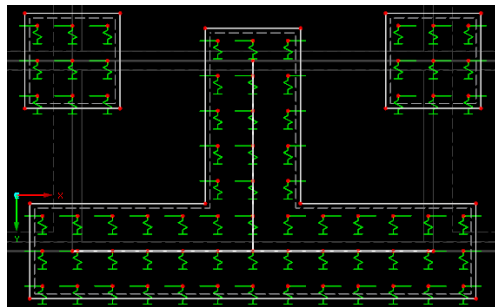


Figure 40: large pile groups

7.5.4 Model 4: Based on a simplification of Model 3

This model will follow the same idea of Model 3 only that the spring distribution was changed and group interaction was considered to all loading directions. For the spring distribution, it will be set equivalent springs on the top of the piles (same idea used in the subgrade reaction approach and shown in Figure 34). The final model looked like Figure 42.

The goal of this model is to analyze if by simplifying Model 3 it is possible to reach equivalent results by using less modeling time.

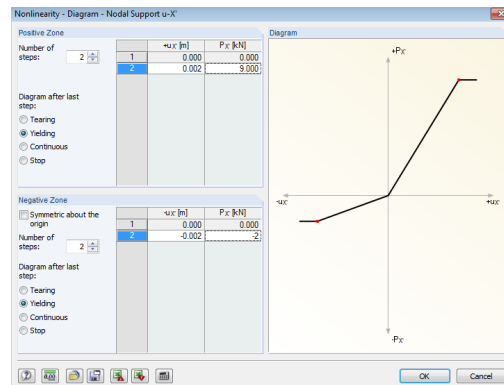


Figure 41: Spring partial activity

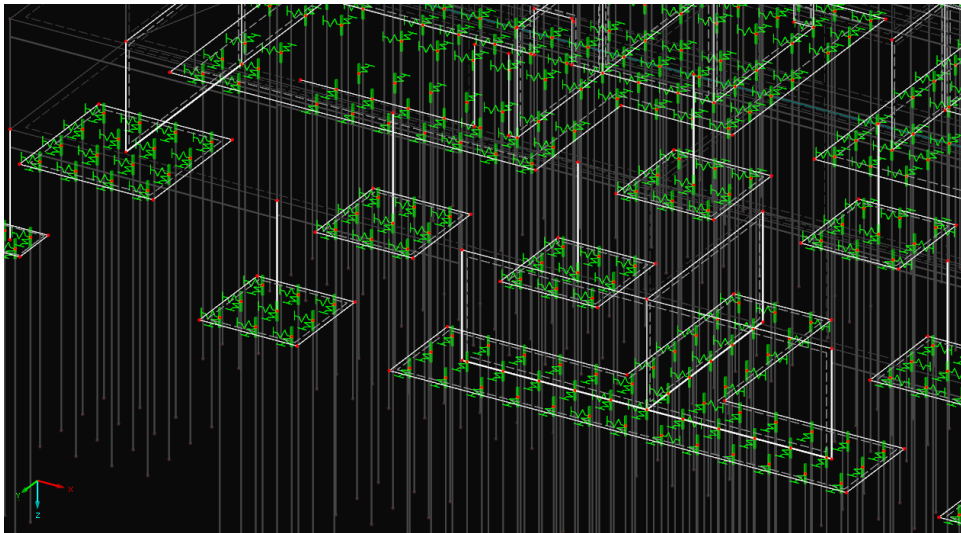


Figure 42: Model 4

8 Results and discussion

In this section it is going to be presented the results of the analysis carried out in the models described above. The results sought on this comparative analysis were the modeling time of the foundation stiffness, the range of results available on each model and the response of the structure for each model.

8.1 Modeling time

The modeling time differed from model to model accordingly to its accuracy. Model 1 will not be commented, since inserting simple supports on several nodes in the model can be done within very short time. Model 2 did not require much time for modeling the springs, since there were only 45 springs in the model. However, it required time to analyze how the resistance of the pile could be taken into account since it was needed to couple piles and model the spring in such a place where it would be effective to all loading sides. Model 3 can take days to be completely modeled if group interaction is considered in all 4 loading directions. In the analysis carried out in this work it was only considered in the positive x and y direction and due to this simplification, springs were reduced from more than two thousand different non linear springs to only 240 linear springs. Modeling 240 different linear springs and setting up their correct places took hours of work. Model 4 was the most time consuming of all models due to the consideration of group interaction in all loading directions. It required around 80 different non-linear springs (for the non-linear spring, see Figure 41, which took more than a full workday to distribute all the springs in the correct places in the model. However, if the same consideration was done in Model 3, it would have been 6 times longer, considering that there were 6 layers of soil.

As a general overview, from fastest to most time taking models, the order was: Model 1, Model 2, Model 4 and Model 3. This taking into account group interaction in all loading directions in Model 3.

8.2 Availability of results for piles

Considering the models which had piles on it, all of them made it possible to check the compression loads on each pile. Horizontal load distribution and bending moment of the piles were available only in some of the models.

In Model 2 it was not possible to analyze the horizontal load distribution or the bending moment on each pile due to the fact the the lateral constraint (the spring) was set in the middle of a pile group. Therefore, the piles were behaving as if they had not lateral forces acting on them. Figure 43 shows the screenshot of the model with bending moment results of members activated, it can be noted that all the values are almost zero on all the piles.

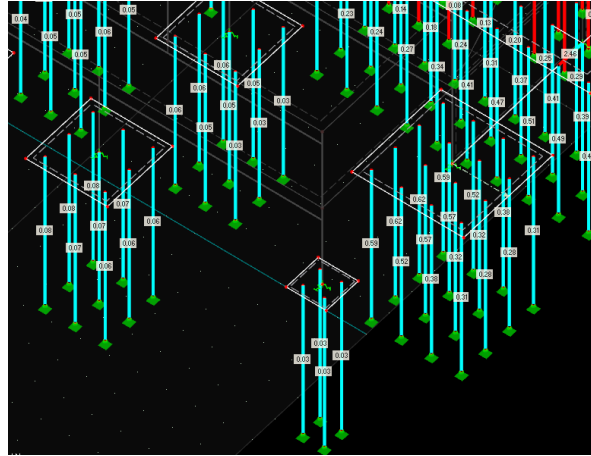


Figure 43: Bending moment of piles, Model 2

Model 3 was the most complete one. As the springs were modeled along the pile shaft, it was closer to the situation on site when soil is supporting the pile linearly, and therefore it was possible to check their bending moment and the force distribution along the pile shaft. See Figure 44 for the bending moment and force distribution along the pile. Analyzing the diagrams on the piles, it can be seen that the internal forces are reduced to zero at certain depth which confirms some of the theories mentioned in the beginning of this work.

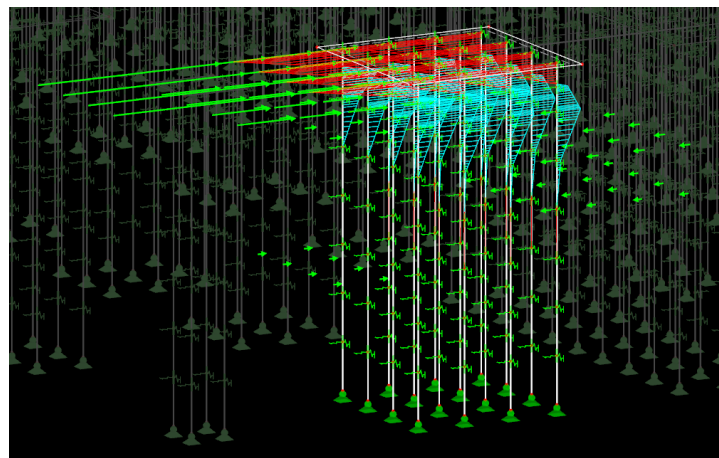


Figure 44: Bending moment of piles, Model 3

Finally, the results available for the piles in Model 4 were similar to Model 2 except that model 4 showed a better horizontal loading distribution due the the fact that each pile had a spring on its head which showed the actual force acting over the pile.

8.3 Other comments concerning modeling and results

When running the calculations in Models 2 and 4 the calculation assistance of the software was informing that there was buckling on the piles of the models. The reason for this is due to the lack of lateral supports along the pile shaft, making the element as a long slender column which will have its critical buckling load reduced to very small values. To overcome this error it was needed to manually reduce the effective length of the piles. However, by doing this the software is hindered to check the buckling modes of the piles in the geometric analysis. This problem did not occur in Model 3, since the pile shaft was laterally supported by springs along, which gave the software enough information to calculate the proper critical buckling mode of the piles.

Another factor in Model 2 was found during the analysis. If there exist any torque around a pile group, the normal case is that it will change the distribution of the horizontal forces on the group. However, as in Model 2 the spring is modeled in the middle of the group this effect would not happen and the torque would be carried by the torsional capacity of the piles.

In this work, the pile lengths were equal throughout the foundation, however, if pile length differs from one place to another, it might change the overall vertical stiffness of the foundation due to the increasing of axial deformation of the piles. This difference in stiffness may affect some of the structural response and needs to be taken into account in the analysis.

8.4 Deformations at foundation level

The variation on the foundation deformation was checked between models. The comparison carried out in this section will take into account Models 2, 3 and 4 and the loading on positive y direction, which was found to be the most critical direction of this structure.

Figures 45, 46 and 47 show the color diagrams of the horizontal deflection of the pile caps of Models 2, 3 and 4 respectively. The range of the values for the color scale had to vary due to the different results between models, which if used the same range would hinder the differential deflection between pile caps on Models 3 and 4. The color range applied to each model can be seen in the label of the figures.

It is noticed that Models 3 and 4 had deflection of very similar magnitude. In the other hand, Model 2 had its maximum horizontal deflection more than 3 times higher when compared to the other models. This might be due to the fact that the pile group resistance was taken into account only by the leading piles, which created a less stiff foundation system when compared to the models that had pile group interaction taken into account, which uses the resistance of every pile within the group.

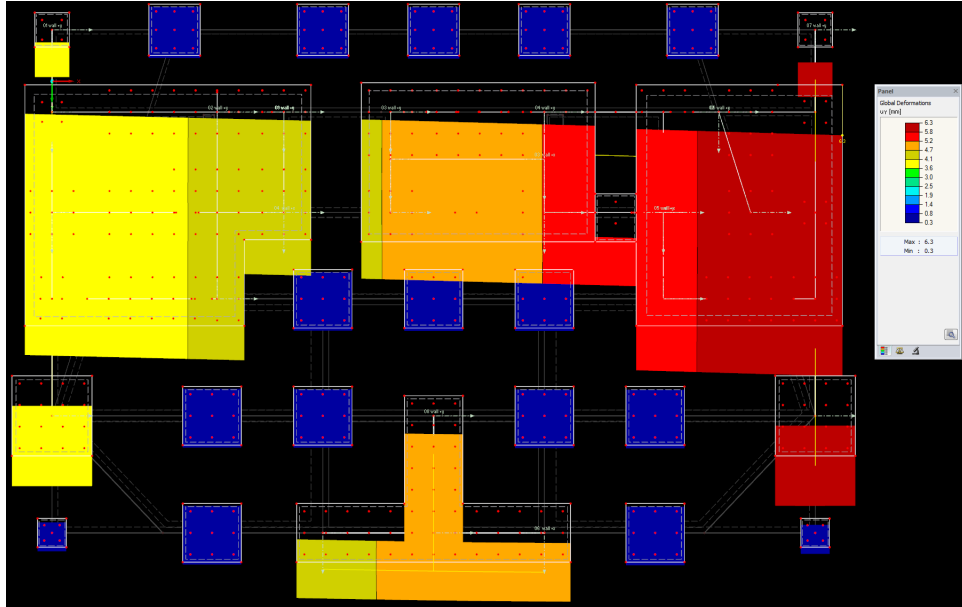


Figure 45: Model 2: deformation on $y+$ (scaling: 0.3-6.3 mm)

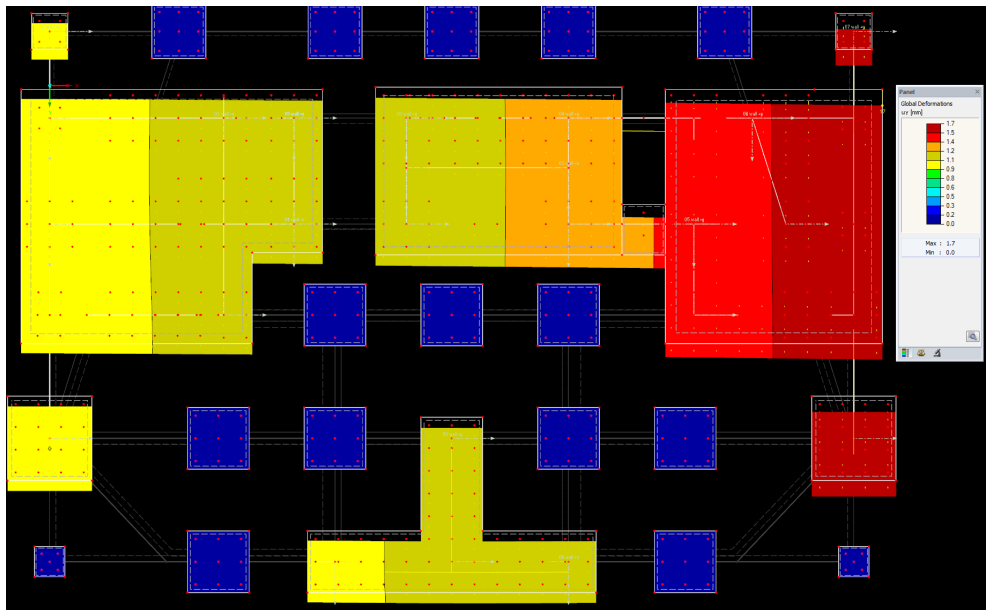


Figure 46: Model 3: deformation on $y+$ (scaling: 0.0-1.7 mm)

8.5 Variation on pile loads

The loads on piles presented in Models 2, 3 and 4 were checked and compared to each other. The biggest variations found were relatively small. the average variation between models 3 and 4 were of 2% and between models 2 and 3 were about 9%.

The loading variation pattern under the big pile caps supporting the shear walls could not be identified. It was noted that it changed as much between Models 2 and

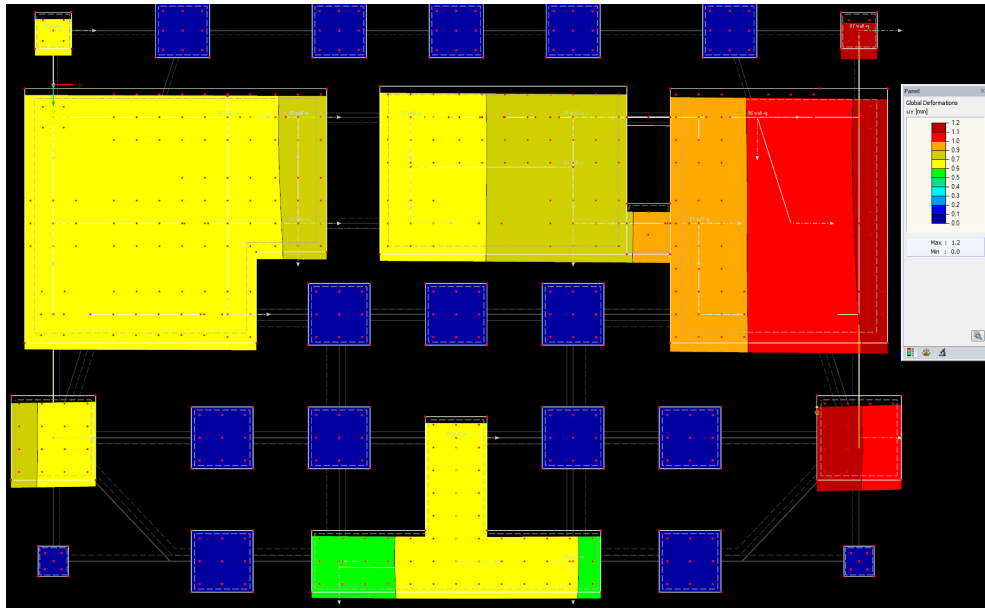


Figure 47: Model 4: deformation on $y+$ (scaling: 0.0-1.2 mm)

3 as between models 3 and 4. However, in small pile caps such as 3x3 piles it was noted that in model 2 the load was shifted from the back pile row to the front pile row. Figure 48 shows two pile caps from Models 2, 3 and 4, it is possible to see that the loading distribution was quite even and equal between models 3 and 4. However, Model 2 has smaller loads on the back piles and higher loads on the front piles of the two pile caps. This shifting of loading may be due to the horizontal deflections of model 2 which are higher than Models 3 and 4.

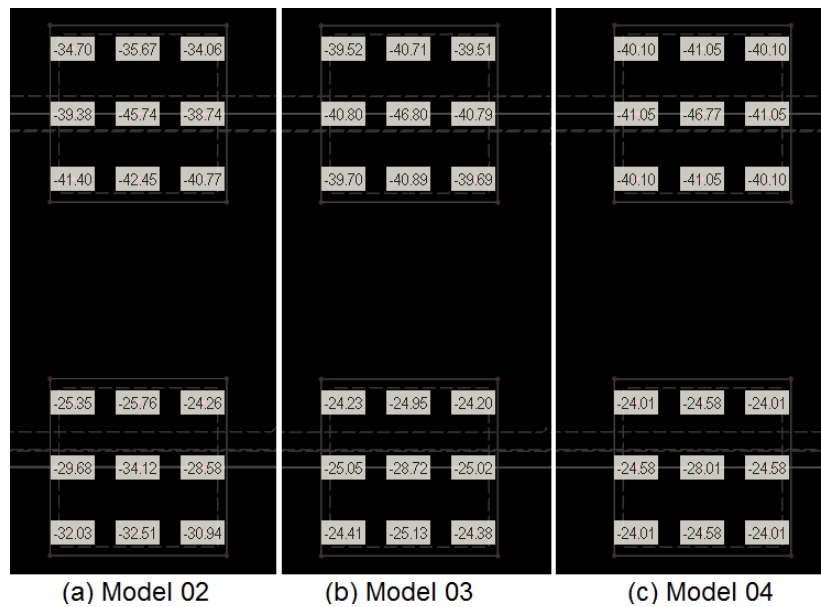


Figure 48: Load distribution on piles

8.6 Lateral loading

It was noted along the analysis of the structure that big lateral loads existent in the model came from structural deformation. For instance, let us analyze one stiffening wall on top of the foundation: Figure 49 shows the deformation of the wall, as vertical loads are bigger in the right side and the vertical stiffness of the foundation allows it to deflects more than the left side, it will create compression zones in a strut and tie fashion that will be transformed in lateral forces in the foundation. If we take the internal stresses from the same wall (see Figure 50) it is possible to see that compression forces were developed in the bottom of the wall and created horizontal loads on the piles.

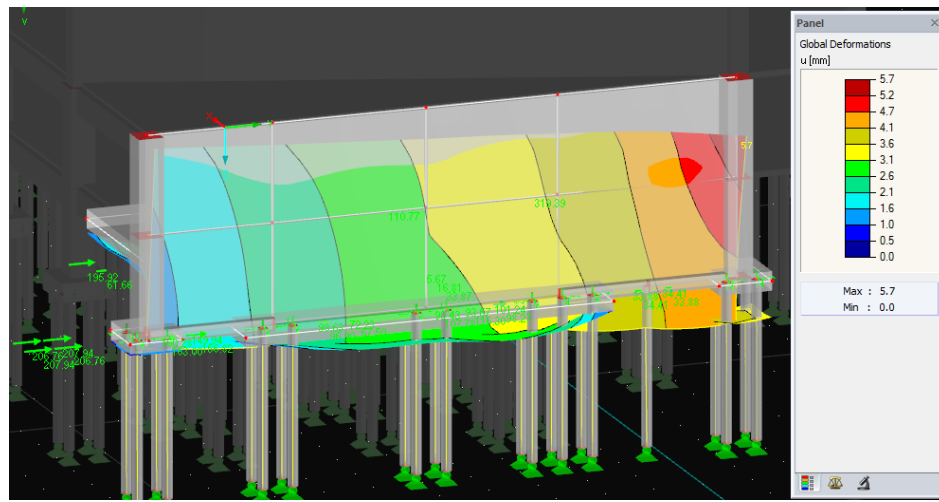


Figure 49: Wall deformation

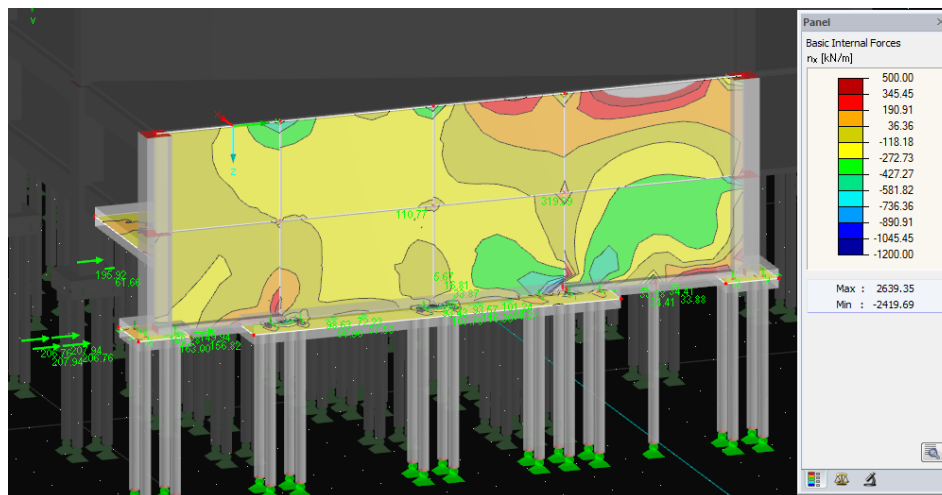


Figure 50: Wall stresses

It was noted that lateral forces reduced its magnitude if the vertical stiffness of the foundation was increased. In the final model, 50% of the average horizontal forces

were due to the vertical loading of the building. This shows that the horizontal and vertical loads are interconnected in the structure.

8.7 Top floor deformations

The deformation of the structure was checked using the Serviceability Limit State load combination. Table 10 shows the deformations of the global directions due to wind loads. Model 3 has no results to negative x and y direction due to the fact the the model received springs for the group effects only on the positive directions. Therefore, the values for the negative directions are not reliable.

Table 10: Global deformations of top floor

Wind direction		+x	+y	-x	-y
Model 1	Global x (mm)	3.0	-2.9	-6.2	-1.1
	Global y (mm)	11.5	29.0	11.5	-4.4
	Global z (mm)	14.8	15.3	14.8	14.8
Model 2	Global x (mm)	5.7	-3.9	-9.5	1.1
	Global y (mm)	12.5	38.3	12.6	-10.2
	Global z (mm)	15.7	16.3	15.8	15.8
Model 3	Global x (mm)	4.3	-3.1		
	Global y (mm)	12.1	34.2		
	Global z (mm)	16.0	16.6		
Model 4	Global x (mm)	4.1	-3.1	-7.4	-1.0
	Global y (mm)	12.2	34.1	12.4	-7.7
	Global z (mm)	16.2	16.8	16.2	16.2

Tables 11 and 12 shows the comparison between the maximum absolute values of each positive global direction. Model 2 had global deformation 90% higher than Model 1 in x direction and 32% in y direction. Comparing Models 3 and 1, these differences were 43% and 18%, while Models 4 and 1 had differences of 37% and 18%. It can be noted that the differences between Models 3 and 4 are relatively small, being 5% for x direction and 0.29% for y direction. This shows that the simplification done in Model 4 did not affect the deformation of the structure. Comparing Model 2 to Models 3 and 4, these differences were higher. Model 2 had top flood deformation of around 35% higher than models 3 and 4 in the positive x direction and 12% higher in positive y direction.

What can be concluded from these deformations is that Model 2 was more flexible than the other Models since group interaction was not taken into account. This higher flexibility on the foundation level increased the deformation of the structure not only on the top floor but also at foundation level. By doing a quick check in the deformation of the foundation it was noted that the lateral deflections of the foundation were on an average more than twice as large as the deflections on Models 3 and 4.

Table 11: Comparison of top floor deformation in positive global x direction

	Model 1	Model 2	Model 3	Model 4
Model 1	0%	90%	43%	37%
Model 2	-47%	0%	-25%	-28%
Model 3	-30%	33%	0%	-5%
Model 4	-27%	39%	5%	0%

Table 12: Comparison of top floor deformation in positive global y direction

	Model 1	Model 2	Model 3	Model 4
Model 1	0%	32%	18%	18%
Model 2	-24%	0%	-11%	-11%
Model 3	-15%	12%	0%	0.29%
Model 4	-15%	12%	0.29%	0%

8.8 Loading distribution on shear walls

All shear walls connecting the structure to the pile caps were checked in all models by its shear forces on the bottom surface of the wall. Firstly, this analysis was carried out by using the Ultimate Limit Load combination, and it was noted that the values of the shear did not change significantly. This might be due to the fact that this structure is quite stiff and the horizontal loading is relatively small when compared to the vertical loading of the structure and therefore it was not possible to see how it affects the global values.

To overcome this problem, the same analysis was performed utilizing only the horizontal loads acting on the structure. By doing this, heavy vertical loads existent in the building would not hinder the affects of horizontal forces. It was noticed then, that the resultant shear values were different to the same wall in the different models. In most of the cases, Models 3 and 4 showed quite similar shear force resultant, with Model 2 having a higher variance both to bigger and smaller values. As some examples, see Figure 51 and 52.

It is safe to say that the sum of the shear force was similar in all the models, however, distributed in different walls. The loading was sometimes transferred to another shear wall in function of the displacement of the foundation. The location of the shear walls 03 and 09 can be viewed in Figure 53, the walls belong to different pile caps which had larger differential deformation in Model 2 when comparing to Models 3 and 4 (see Figures 45, 46 and 47). The differential deflection between the two pile caps was concluded to be the factor transferring loading from one wall to another. The biggest difference between Model 1 to the other models is due to the complete

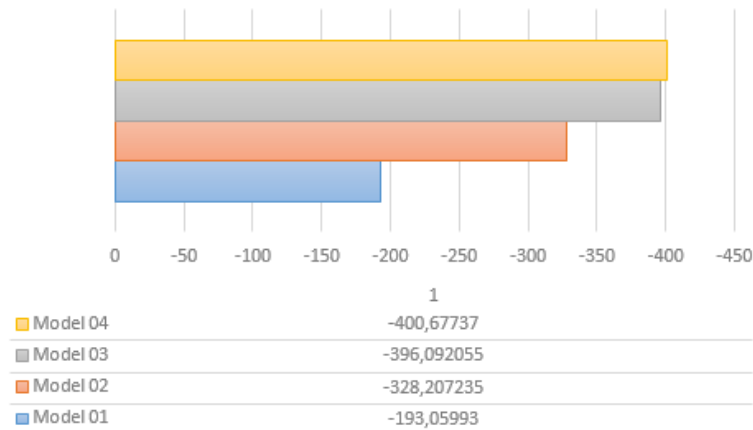


Figure 51: shear resultant +y direction: Shear wall 03

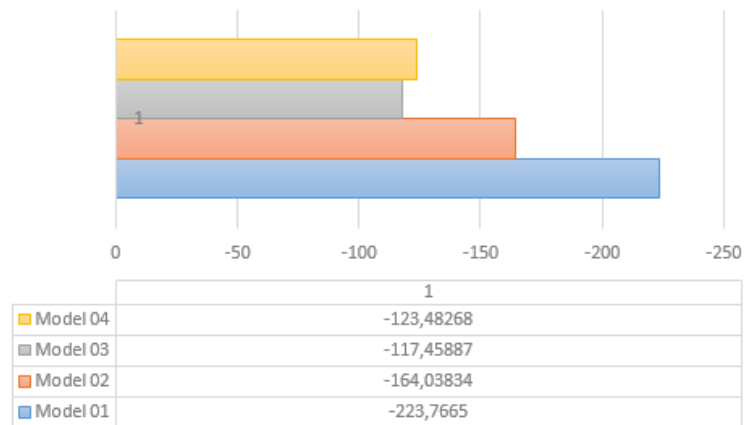


Figure 52: shear resultant +y direction: Shear wall 09

restrain of the model, which does not allow deformation to occur.

If the structure analyzed on this work was less stiff, the effects explained above could be increased to significant values and could play an important role in design. If the stiffness of the foundation is not correctly implemented in structural analysis, the reinforcement between shear walls and foundation may be under or over designed, which may lead to structural failures. Based on these results, it can be said that it is of high importance to model correctly the soil-foundation stiffness to obtain a more accurate load distribution on the structural elements.

8.9 Natural frequency

The first three modes of the natural frequency of the structure were check on each model as additional results of this study.

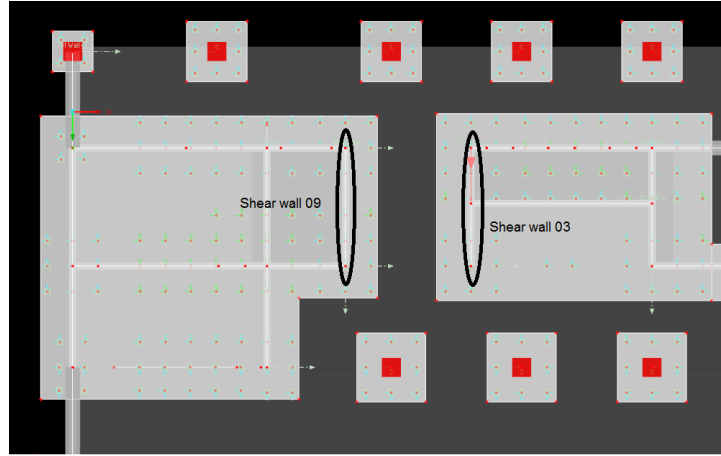


Figure 53: Location of shear walls 03 and 09

Model 1 had the highest frequencies on all three modes, which was expected due to its rigid support. Model 2 had higher frequencies than Model 3 and Model 4 in the first and second mode and intermediate frequency in the third mode when compared to Models 3 and 4. This behavior does not follow the concept that due to its more flexible foundation, Model 2 should have the lowest frequencies than the other models. The pattern of these alterations was not identified in this study.

Table 13: Natural frequency

	First mode	Second mode	Third mode
Model 1	0.616Hz	0.842Hz	1.482Hz
Model 2	0.523Hz	0.645Hz	0.892Hz
Model 3	0.470Hz	0.549Hz	0.857Hz
Model 4	0.416Hz	0.572Hz	0.933Hz

9 Conclusion

The results of this research made it possible to draw several conclusions of soil-structure interaction and how the structure behaves in each lateral stiffness model. These results will help to improve future structural analysis of different structures and also the interaction between structural and geotechnical engineers. The principal points that were taken from the main results are listed below:

- The soil-foundation model affects the response of the structure on top of it;
- The lateral stiffness of the foundation influences the horizontal deflection of the building;
- The lateral stiffness of the foundation influences the loading distribution both in the load bearing structure as well as in the piles;
- The lateral stiffness of foundation is dependent on the horizontal deflection of the foundation elements;
- Considering pile group interaction may increase the stiffness of the foundation when compared to considering only leading rows. This can wider the range of situations where raked piles can be avoided;
- The vertical stiffness of foundation is a factor that can alter the horizontal loads and can also create significant horizontal load at foundation level if not controlled;
- The vertical stiffness of foundation also contributes to top horizontal deflection of building.

Based on these points, it can be added that modeling the real length and the cross-section of piles is of extreme importance in order to get closer to real results from the structural models. The placing of piles should also be considered by the vertical deflection of the piles and not only by load bearing capacity, like this it is possible to control better the deflections of the structure and avoid unnecessary loads created by the deflection of load bearing elements in the boundary between foundation and the superstructure.

Another important factor that can be drawn from the results is that the lateral stiffness of the foundation should be calculated in accordance with real lateral displacements in the model. This is an interactive process and therefore the cooperation between structural and geotechnical engineer comes into play to solve this matter.

The research carried out on this work also brought into light some situations in which engineers should be extremely careful if they are coming into the analysis, these situations are listed as follow:

- When large displacements are taking place at the foundation leading to plastic strain of the soil;
- When foundation is on very soft soils such as soft clay, which are prone to flow around the pile and/or consolidate easily;
- Since the experimental researches on pile group interaction were mostly performed on granular soils and over-consolidated clays, the coefficients of group interaction presented on this work should be considered carefully when dealing with very soft soils and soft clays.

The limits of the factors just mentioned above should be discussed with the geotechnical designer, since each soil has its own behavior and limitations. These points, however, bring awareness into structural offices of the situations that require a more careful analysis. If those factors are not clearly answered by geotechnical analysis, raked pile is recommended for a safer design.

9.1 Applications of the Models

The models studies in this work may be applicable to different structures and recommendations are going to be done in the following. The idea is to clarify in which situations each model can be applied, their advantages and disadvantages.

Model 1

May be suitable for structures directly on bed rock or for very small structures where soil-foundation interaction will not be important for the results (may be a very fictional case). May as well be used to double check stability hand calculations. Advantages are the fast and easy modeling. Disadvantage is that deformation is not allowed in the supports.

Model 2

May be suitable when variation of the internal forces of the load bearing elements is not a risk to the design (this can be accessed by a pre-design) and when there is no twisting moments on the foundation. Advantages are the fast modeling time and the simplicity of the modeling. Disadvantages are that it is not possible to check all internal forces of the piles and does not simulate the real stiffness of soil-foundation interaction.

Model 3

May be suitable to any structure, but specially to very large structural systems where variations of results can be a risk. Advantages is that it is supposed to give the most precise results and all internal forces and force distribution on the piles can be accessed. Disadvantages are that it is very time consuming and can be very complicated to model.

Model 4

May be suitable to large structures assumed that the simplification is not a risk. Advantages are that it shows close results to Model 3 and is simpler to model. Disadvantages are that it does not show the load distribution on the pile shaft and the bending moment on the piles.

If working with a very soft soil, it is possible that Model 3 is the only recommended since it is possible to model each layer of spring in a different way, this could allow the top springs to be modeled with an initial slip to simulate the gaping. Model 3 is also recommended to models where checking the bending moments of the piles is an important factor in design.

9.2 Cooperation between structural and geotechnical engineers

A list of starting information each field would require will be suggested here. It is also important to go through this list in a meeting before the start of the calculations so that both geotechnical and structural engineers can discuss about additional information of what is needed to the specific project.

What geotechnical engineers need to know at preliminary stages

- Limiting horizontal deflection at foundation level so that pile deflection is estimated;
- What type of structure is on top of the foundation and what is the precision of the analysis needed;
- What types of foundation systems are available;
- Magnitude of loading at foundation level.

What structural engineers need to know at preliminary stages

- limiting pressure along the pile shaft with their corresponding displacement;
- What was the nature of the analysis run (static, cyclic, dynamic);
- What are the limits to avoid plastic deformations on the soil after some years;
- Recommendations of spring models for the soil;
- Recommendations of foundation systems;
- Recommendations if pile cap should be considered as part of the resistance of the foundation.

Coordination at later stages

The sharing of information between the two fields should not stop after the information on the preliminary stages are given. It is important that results from structural analysis with the soil-foundation stiffness are shared with geotechnical designers so that they can confirm if the results are accordingly to their analysis. For this, meeting are recommended in the later stages of the project in order to check results and exchange further recommendations until risks and misleading results are minimized.

9.3 Final comments

Overall, the results of this study made it more clear on how the modeling of the lateral stiffness of the foundation affects the structural analysis. A cooperation between structural and geotechnical engineers was proposed making it more clear how both field should interact to each other. And finally, structural engineers are now able to understand and identify the risks they are taking when using each models suggested in this work.

Suggestion of the continuation of this work were developed along this research, some of the ideas are going to be itemized bellow:

- How the stiffness of the building affects the results found on this work?
- How should the modeling be done for large pile deflections, where gaping is present between soil and pile?

References

- [1] Al-Shamary, J. M. A., Chik, Z., Taha, M. R. (2018) 'Modeling the lateral response of pile groups in cohesionless and cohesive soils' *International Journal of Geo-Engineering*, 9(1): 1-17. Retrieved from: ASCE [Accessed on 27 May 2018]
- [2] Bowles, J. E. (1997) *Foundation analysis and design* Fifth edition. Singapore: McGraw-Hill. 1175 p. ISBN 0-07-912247-7.
- [3] Brown, D. A., Reese, L. C., O'Neill, M. W., (1987) 'Cyclic lateral loading of a large-scale pile group' *Journal of Geotechnical Engineering*, 113(11): 1326-1343. Retrieved from: ASCE [Accessed on 28 May 2018]
- [4] Brown, D. A., Morrison, C., Reese, L. C., (1988) 'Lateral load behavior of pile groups in sand' *Journal of Geotechnical Engineering*, 114(11): 1261-1276. Retrieved from: ASCE [Accessed on 21 May 2018]
- [5] Brown, D. A., and Shie, C-F, (1991) 'Modification of p-y curves to account for group effects on laterally loaded piles' *Geotechnical Special Publications*, 1(27): 479-490. Retrieved from: ResearchGate [Accessed on 28 May 2018]
- [6] Calgaro, J. A., Gulvanessian, H. and Formichi, P. (2013) *Calcul des actions sur les bâtiments selon l'Eurocode 1 (Designers' guide to Eurocode 1 : actions on buildings)* First edition. Paris: Le Moniteur. 366 p. ISBN 978-2-281-11606-9.
- [7] Cernica, J. N. (1995) *Geotechnical Engineering: Foundation design* First edition. USA: Jhon Wiley e sons, Inc. 486 p.
- [8] Coduto, D. P. (2001) *Foundation Design: Principles and Practices* Second edition. USA: Prentice-Hall, Inc. 881 p. ISBN 0-13-589706-8.
- [9] Edgers, L., Sanayei, M., Along, J. L. (2005) 'Modeling the effects of soil-structure interaction on a tall building bearing on a mat foundation' *Civil Engineering Practice*, 20(2): 51-68. Retrieved from: ResearchGate [Accessed on 25 June 2018]
- [10] Elhakim, A. F., Khouly, M. A. A. E., Awad, R. (2014) 'Three dimensional modeling of laterally loaded pile groups resting in sand' *Housing and Building Research Center journal*, 12: 78-87. Retrieved from: Elsevier [Accessed on 21 May 2018]
- [11] Fleming, W. G. K., Weltman, A. J., Randolph, M. F., Elson, W. K. (1992) *Piling Engineering* Second edition. Glasgow : New York : Blackie. Wiley. 390 p.
- [12] Liikennevirasto. (2012) *Sillan geotekninen suunnittelu. Liikenneviraston ohjeita 11/2012 (Geotechnical design of bridges. Instructions from the Finnish Transport Agency 11/2012)*. Helsinki, FI:Helsinki: Liikennevirasto. ISBN 978-952-255-143-6.

- [13] McVay, M., Zhang, L., Molnit, T., Lai, P. (1998) 'Centrifuge testing of large laterally loaded pile groups in sands' *Journal of Geotechnical and Geoenvironmental Engineering*, 124(10): 1016-1026. Retrieved from: ASCE [Accessed on 24 May 2018]
- [14] Niiranen, J. (2017) *Finite Element Methods in Civil Engineering*. Aalto University. Lecture notes.
- [15] O'Reilly, M. P., Brown, S. F. (2006) *Cyclic Loading of Soils : from theory to design*. Glasgow and London, New York: Blackie, Van Nostrand Reinhold. 475 p. ISBN 0-216-92898-2.
- [16] Poulos, H. G. (2014) 'Challenges in the Design of Tall Building Foundations' *Geotechnical Engineering Journal of the SEAGS & AGSSEA*, Vol. 45 No. 4. Retrieved from: <https://www.researchgate.net/publication/273949144> [Accessed on 06 July 2018]
- [17] Poulos, H. G.; Davis, E. H. (1980) *Pile Foundation Analysis and Design*. Wiley, New York.
- [18] Puech, A. (2013) 'Design for cyclic loading: piles and other foundations' *Proceedings of TC 209 workshop*; Paris, France, 4 September 2013. P. 93.
- [19] Philipponnat, G., Hubert, B. (2006) *Fondation et ouvrages en terre (Foundation and soil works)*. Tenth edition. Paris: Eyrolles. 548 p. ISBN 978-2-212-14487-1.
- [20] Rao, S. S. (1999) *The Finite Element Method in Engineering*. Third edition. USA: Butterworth-Heinemann. 559 p. ISBN 0-7506-7072-X.
- [21] Rasi-Koskinen, H. (2014) *Vaakasuuntaiset alustaluvut paaluperusteisissa silloissa (Horizontal modulus of subgrade reaction in pile-founded bridges)*. M.A. Dissertation. Oulu, FI: Oulu University [published].
- [22] Reese, L. C.; Isenhower, W. M., Wang, S. T.. K. (2006) *Analysis and design of shallow and deep foundations*. USA: John Wiley & sons. 574 p. ISBN 978-0-471-43159-6.
- [23] RIL 212-2001. (2011) *Suurpaalutusohje (XXXI)*. Helsinki, FI: Suomen Rakennusinsinöörien Liitto RIL ry. 150 p. ISBN 951-759-412-1.
- [24] RIL 254-2011. (2011) *Paalutusohje (Piling manual)*. Helsinki, FI: Suomen Rakennusinsinöörien Liitto RIL ry. 260 p. ISBN 978-951-758-528-6.
- [25] Rollins, K. M., Olsen, K. G., Jensen, D. H., Garrett, B. H., Olsen, R. J., Egbert, J. J., (2006) 'Pile Spacing Effects on Lateral Pile Group Behavior: Analysis' *Journal of Geotechnical and Geoenvironmental Engineering*, 132(10): 1272-1283. Retrieved from: ASCE [Accessed on 27 May 2018]

- [26] Salgado, R., Tehrani, F. S., Prezzi, M. (2014) 'Analysis of laterally loaded pile groups in multilayered elastic soil' *Computers and Geotechnics*, 62: 136-153. Retrieved from: Elsevier [Accessed on 21 May 2018]
- [27] Tuotelehti: Suunnittelu, työmaatoiminta ja paalujen valmistus (Product sheet: Design, construction site and pile manufacturing) (2011) Available from: https://htmyhtiot.fi/assets/files/pdf/paalutuotelehti_RT2011.pdf [Accessed on 16 July 2018]
- [28] Smith, B. S., Coull, A. (1991) *Tall Building Structures: Analysis and Design*. USA: Wiley-Interscience. 537 p. ISBN 0-471-51237-0.
- [29] Snyder, J. L., (2004) *Full-Scale Lateral Load Tests of a 3x5 Pile Group in Soft Clays and Silts*. M.A. Dissertation. USA, Brigham Young University.
- [30] Stewart, J. P., Crouse, C. B., Hutchinson, T., Lizundia, B., Naeim, F., Ostadan, F. (2012) *Soil-Structure Interaction for Building Structures*. Available from: <https://www.nist.gov/publications/soil-structure-interaction-building-structures> [Accessed on 13 June 2018]
- [31] SFS-EN 1990. *Eurocode 0: Bases of structural design*. Helsinki: Finnish Standards Association. 2000. 87p.
- [32] SFS-EN 1991. *Eurocode 1: Actions on structures. Part 1-1: General actions. Densities, self-weight, imposed loads for buildings* Helsinki: Finnish Standards Association. 2002. 44p.
- [33] SFS-EN 1991. *Eurocode 1: Actions on structures. Part 1-3: General actions. Snow loads* Helsinki: Finnish Standards Association. 2004. 56p.
- [34] SFS-EN 1991. *Eurocode 1: Actions on structures. Part 1-4: General actions. Wind actions* Helsinki: Finnish Standards Association. 2011. 254p.
- [35] Terzaghi, K. (1995) *Evaluation of coefficients of subgrade reaction*. Geotechnique, Vol. 5, No. 4, 41-50. Pages 297-326.
- [36] Tomlinson, M. J. (2001) *Foundation Design and Construction* Seventh edition. Harlow: Pearson Education. 569 p. ISBN 978-0-13-031180-1.
- [37] Virtanen, E. (2015) *Assessment of vibration control criteria for tall buildings*. M.A. Dissertation. Espoo, FI: Aalto University.
- [38] Walsh, J. M., (2005) *Full-Scale Lateral Load Test of a 3x5 Pile Group in Sand*. M.A. Dissertation. USA, Brigham Young University.

A Annex 01

Tables for assessing strength and deformation properties of soil layers on the basis of resistance (Translated from: Finnish Traffic Agency 2012).

Soil type		Volume weight (kN/m ³)		Friction angle (°)	Janbu's modification parameters		Sounding resistance from borehole log		
		Bellow ground water	Above ground water		Modulus m	Tension exponent β	Cone penetration test q_c (MPa)	Weight sounding Pk/0.2 m	Ram drilling L/0.2 m
Coarse silt	Loose	14 ... 16	9 ...	28	30 ... 100	0,3	< 7	< 40	< 8
	Medium dense			30	70 ... 150	0,3	7 ... 15	40 ... 100	8 ... 25
	Dense	16 ... 18	11	32	100 ... 300	0,3	> 15	> 100	> 25
Fine sand $d_{10}<0,06$	Loose	15 ... 17	9 ...	30	50 ... 150	0,5	< 10	20 ... 50	5 ... 15
	Medium dense			33	100 ... 200	0,5	10 ... 20	50 ... 100	15 ... 30
	Dense	16 ... 18	11	36	150 ... 300	0,5	> 20	> 100	> 30
Sand $d_{10}>0,06$	Loose	16 ... 18	10 ...	32	150 ... 300	0,5	< 6	10 ... 30	5 ... 12
	Medium dense			35	200 ... 400	0,5	6 ... 14	30 ... 60	12 ... 25
	Dense	18 ... 20	12	38	300 ... 600	0,5	> 14	> 60	> 25

Soil type		Volume weight (kN/m ³)		Friction angle (°)	Janbu's modification parameters		Sounding resistance from borehole log		
		Bellow ground water	Above ground water		Modulus m	Tension exponent β	Cone penetration test q_c (MPa)	Weight sounding Pk/0.2 m	Ram drilling L/0.2 m
Gravel	Loose	17 ... 19	10 ...	34	300 ... 600	0,5	< 5,5	10 ... 25	5 ... 10
	Medium dense			37	400 ... 800	0,5	5,5 ... 12	25 ... 50	10 ... 20
	Dense	18 ... 20	12	40	600 ... 1200	0,5	> 12	> 50	> 20
Moraine	Very loose	16 ... 19	10 ... 12	... 34	(≤ 100)* 300 ... 600	0,5	< 10	< 40	< 20
	loose	17 ... 20	10 ... 12	... 36	(100...250)* 600 ...	0,5	> 10	40 ... 100	20 ... 60
	Medium dense	18 ... 21	11 ... 13	... 38	800 ...	0,5	-	> 100	60 ... 140
	Dense	19 ... 23	11 ... 14	... 40	1200 ...	0,5	-	By hitting	> 140

*) If moraine has not been squeezed by the glacier

B Annex 02

Terrain categories and terrain parameters. Table 4.1 EN 1991-1-4

Terrain category		z_0 m	z_{min} m
0	Sea or coastal area exposed to the open sea	0,003	1
I	Lakes or flat and horizontal area with negligible vegetation and without obstacles	0,01	1
II	Area with low vegetation such as grass and isolated obstacles (trees, buildings) with separations of at least 20 obstacle heights	0,05	2
III	Area with regular cover of vegetation or buildings or with isolated obstacles with separations of maximum 20 obstacle heights (such as villages, suburban terrain, permanent forest)	0,3	5
IV	Area in which at least 15 % of the surface is covered with buildings and their average height exceeds 15 m	1,0	10
NOTE: The terrain categories are illustrated in A.1.			

C Annex 03

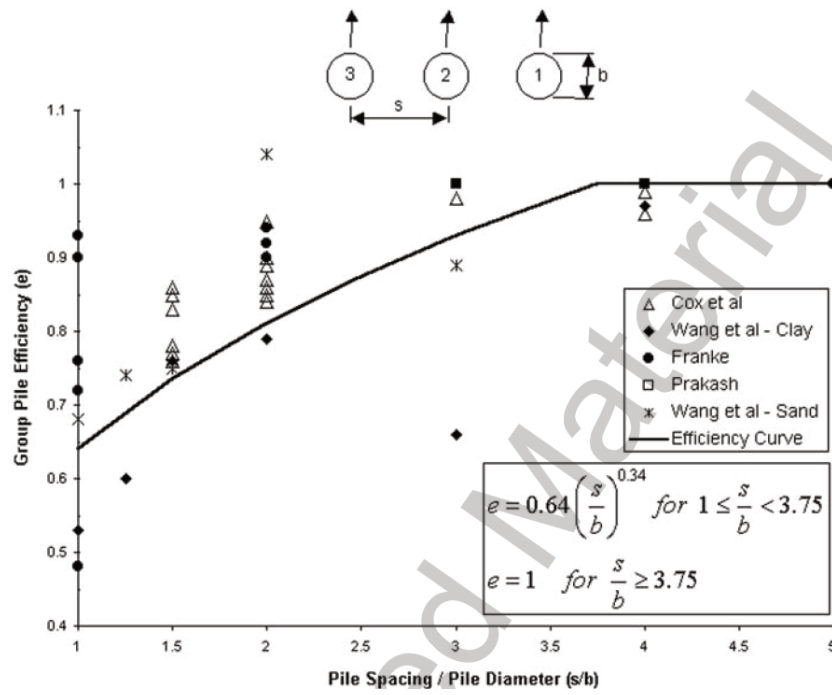


Figure C1: Side-by-side piles [22]

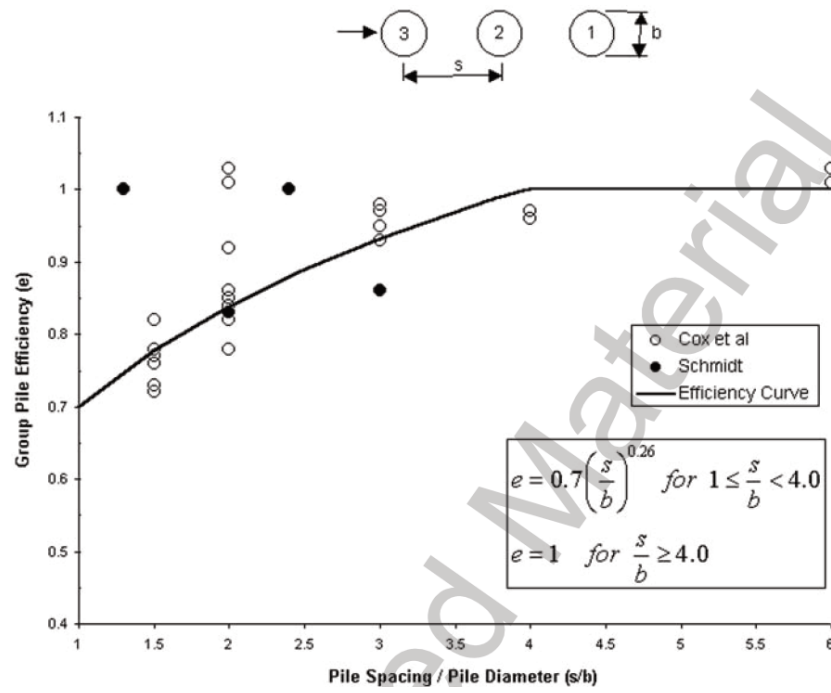


Figure C2: Line-by-line piles, leading piles [22]

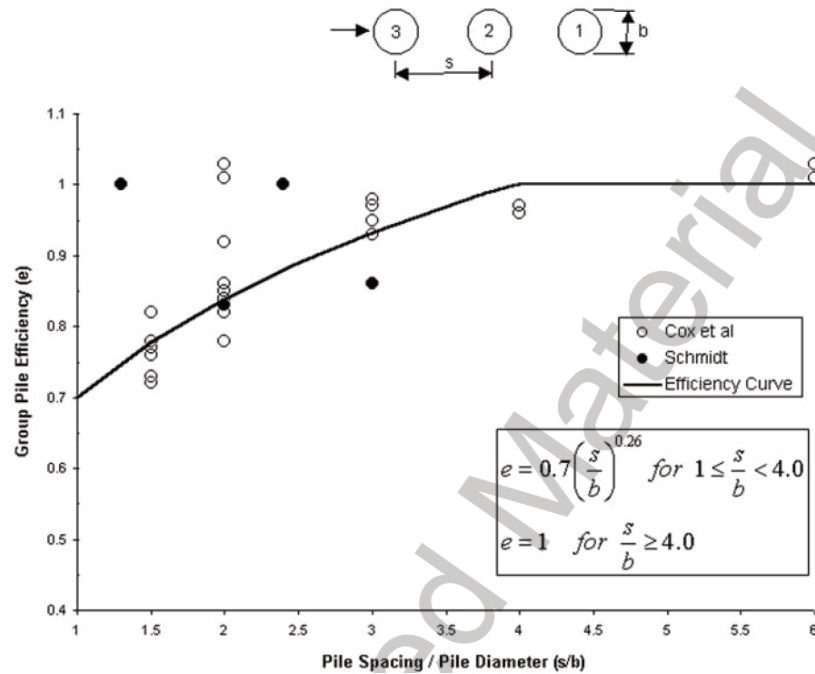
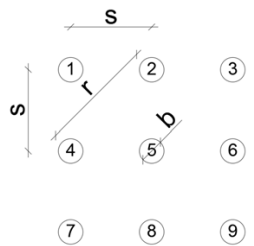


Figure C3: Line-by-line piles, trailing piles [22]

Pile group representation and reduction equations



$$e_{\text{side}} := 0.65 \cdot \left(\frac{s}{b} \right)^{0.34} \quad 1 \leq \frac{s}{b} \leq 3.75 \quad \text{otherwise} \quad e_{\text{side}} := 1$$

$$e_{\text{leading}} := 0.70 \cdot \left(\frac{s}{b} \right)^{0.26} \quad 1 \leq \frac{s}{b} \leq 4.0 \quad \text{otherwise} \quad e_{\text{side}} := 1$$

$$e_{\text{trailing}} := 0.48 \cdot \left(\frac{s}{b} \right)^{0.38} \quad 1 \leq \frac{s}{b} \leq 7.0 \quad \text{otherwise} \quad e_{\text{side}} := 1$$

$$e_{\text{skewed}} := \left(e_{\text{line}}^2 \cdot \cos(\theta)^2 + e_{\text{side}}^2 \cdot \sin(\theta)^2 \right)^{\frac{1}{2}}$$

Assembling reduction factors for each pile

$$f_1 := e_{\text{side_21}} \cdot e_{\text{leading_41}} \cdot e_{\text{skewed_leading_51}}$$

$$f_2 := e_{\text{side_12}} \cdot e_{\text{side_32}} \cdot e_{\text{leading_52}} \cdot e_{\text{skewed_leading_42}} \cdot e_{\text{skewed_leading_62}}$$

$$f_3 := e_{\text{side_23}} \cdot e_{\text{leading_63}} \cdot e_{\text{skewed_leading_53}}$$

$$f_4 := e_{\text{side_54}} \cdot e_{\text{leading_74}} \cdot e_{\text{trailing_14}} \cdot e_{\text{skewed_leading_84}} \cdot e_{\text{skewed_trailing_24}}$$

$$f_5 := e_{\text{side_45}} \cdot e_{\text{side_65}} \cdot e_{\text{leading_85}} \cdot e_{\text{trailing_25}} \cdot e_{\text{skewed_leading_75}} \cdot e_{\text{skewed_leading_95}} \cdot e_{\text{skewed_trailing_15}} \cdot e_{\text{skewed_trailing_35}}$$

$$f_6 := e_{\text{side_56}} \cdot e_{\text{leading_96}} \cdot e_{\text{trailing_23}} \cdot e_{\text{skewed_leading_86}} \cdot e_{\text{skewed_trailing_26}}$$

$$f_7 := e_{\text{side_87}} \cdot e_{\text{trailing_47}} \cdot e_{\text{skewed_trailing_57}}$$

$$f_8 := e_{\text{side_78}} \cdot e_{\text{side_98}} \cdot e_{\text{trailing_58}} \cdot e_{\text{skewed_trailing_48}} \cdot e_{\text{skewed_trailing_68}}$$

$$f_9 := e_{\text{side_89}} \cdot e_{\text{trailing_69}} \cdot e_{\text{skewed_trailing_59}}$$

Calculating the p-multipliers for $s/b=3D$ and $s/b=3.92D$

$$\text{FOR: } \frac{s}{b} := 3 \quad \theta := 1 \quad r := \sqrt{2} \cdot s \quad \frac{r}{b} = 4.243$$

Reduction coefficients

$$e_{\text{side}} := 0.65 \cdot \left(\frac{s}{b} \right)^{0.34} = 0.944$$

$$e_{\text{leading}} := 0.70 \cdot \left(\frac{s}{b} \right)^{0.26} = 0.931$$

$$e_{\text{trailing}} := 0.48 \cdot \left(\frac{s}{b} \right)^{0.38} = 0.729$$

Reduction coefficients for skewed

$$e_{\text{side_skewed}} := 1$$

$$e_{\text{leading_skewed}} := 1$$

$$e_{\text{trailing_skewed}} := 0.48 \cdot \left(\frac{r}{b} \right)^{0.38} = 0.831$$

$$e_{\text{skewed_leading}} := \left(e_{\text{leading_skewed}}^2 \cdot \cos(\theta)^2 + e_{\text{side_skewed}}^2 \cdot \sin(\theta)^2 \right)^{\frac{1}{2}} = 1$$

$$e_{\text{skewed_trailing}} := \left(e_{\text{trailing_skewed}}^2 \cdot \cos(\theta)^2 + e_{\text{side_skewed}}^2 \cdot \sin(\theta)^2 \right)^{\frac{1}{2}} = 0.954$$

Assembling p-multipliers

$$\begin{aligned}
f_1 &:= e_{\text{side}} \cdot e_{\text{leading}} \cdot e_{\text{skewed_leading}} = 0.88 \\
f_2 &:= e_{\text{side}}^2 \cdot e_{\text{leading}} \cdot e_{\text{skewed_leading}} \cdot e_{\text{skewed_leading}} = 0.831 \\
f_3 &:= e_{\text{side}} \cdot e_{\text{leading}} \cdot e_{\text{skewed_leading}} = 0.88 \\
f_4 &:= e_{\text{side}} \cdot e_{\text{leading}} \cdot e_{\text{trailing}} \cdot e_{\text{skewed_leading}} \cdot e_{\text{skewed_trailing}} = 0.611 \\
f_5 &:= e_{\text{side}}^2 \cdot e_{\text{leading}} \cdot e_{\text{trailing}} \cdot e_{\text{skewed_leading}}^2 \cdot e_{\text{skewed_trailing}}^2 = 0.551 \\
f_6 &:= e_{\text{side}} \cdot e_{\text{leading}} \cdot e_{\text{trailing}} \cdot e_{\text{skewed_leading}} \cdot e_{\text{skewed_trailing}} = 0.611 \\
f_7 &:= e_{\text{side}} \cdot e_{\text{trailing}} \cdot e_{\text{skewed_trailing}} = 0.656 \\
f_8 &:= e_{\text{side}}^2 \cdot e_{\text{trailing}} \cdot e_{\text{skewed_trailing}}^2 = 0.591 \\
f_9 &:= e_{\text{side}} \cdot e_{\text{trailing}} \cdot e_{\text{skewed_trailing}} = 0.656
\end{aligned}$$

Estimation of efficiency per row of piles

$$\begin{aligned}
\text{Row 01} \quad & \frac{f_1 + f_2 + f_3}{3} = 0.863 \\
\text{Row 02} \quad & \frac{f_4 + f_5 + f_6}{3} = 0.591 \\
\text{Row 03} \quad & \frac{f_7 + f_8 + f_9}{3} = 0.635
\end{aligned}$$

$$\text{FOR: } \frac{s}{b} := 3.92 \quad \frac{\theta}{\alpha} := 1 \quad r := \sqrt{2} \cdot s \quad \frac{r}{b} = 5.544$$

Reduction coefficients

$$\begin{aligned}
e_{\text{side}} &:= 1 \\
e_{\text{leading}} &:= 0.70 \left(\frac{s}{b} \right)^{0.26} = 0.999 \\
e_{\text{trailing}} &:= 0.48 \left(\frac{s}{b} \right)^{0.38} = 0.807
\end{aligned}$$

Reduction coefficients for skewed

$$\begin{aligned}
e_{\text{side_skewed}} &:= 1 \\
e_{\text{leading_skewed}} &:= 1 \\
e_{\text{trailing_skewed}} &:= 0.48 \left(\frac{r}{b} \right)^{0.38} = 0.92 \\
e_{\text{skewed_leading}} &:= \left(e_{\text{leading_skewed}}^2 \cdot \cos(\theta)^2 + e_{\text{side_skewed}}^2 \cdot \sin(\theta)^2 \right)^{\frac{1}{2}} = 1 \\
e_{\text{skewed_trailing}} &:= \left(e_{\text{trailing_skewed}}^2 \cdot \cos(\theta)^2 + e_{\text{side_skewed}}^2 \cdot \sin(\theta)^2 \right)^{\frac{1}{2}} = 0.977
\end{aligned}$$

Assembling p-multipliers

$$\begin{aligned}
f_1 &:= e_{\text{side}} \cdot e_{\text{leading}} \cdot e_{\text{skewed_leading}} = 0.999 \\
f_2 &:= e_{\text{side}}^2 \cdot e_{\text{leading}} \cdot e_{\text{skewed_leading}} \cdot e_{\text{skewed_leading}} = 0.999 \\
f_3 &:= e_{\text{side}} \cdot e_{\text{leading}} \cdot e_{\text{skewed_leading}} = 0.999 \\
f_4 &:= e_{\text{side}} \cdot e_{\text{leading}} \cdot e_{\text{trailing}} \cdot e_{\text{skewed_leading}} \cdot e_{\text{skewed_trailing}} = 0.787
\end{aligned}$$

$$f_{5.5} := e_{\text{side}}^2 \cdot e_{\text{leading}} \cdot e_{\text{trailing}} \cdot e_{\text{skewed_leading}}^2 \cdot e_{\text{skewed_trailing}}^2 = 0.769$$

$$f_{6.5} := e_{\text{side}} \cdot e_{\text{leading}} \cdot e_{\text{trailing}} \cdot e_{\text{skewed_leading}} \cdot e_{\text{skewed_trailing}} = 0.787$$

$$f_{7.5} := e_{\text{side}} \cdot e_{\text{trailing}} \cdot e_{\text{skewed_trailing}} = 0.788$$

$$f_{8.5} := e_{\text{side}}^2 \cdot e_{\text{trailing}} \cdot e_{\text{skewed_trailing}}^2 = 0.771$$

$$f_{9.5} := e_{\text{side}} \cdot e_{\text{trailing}} \cdot e_{\text{skewed_trailing}} = 0.788$$

Estimation of efficiency per row of piles

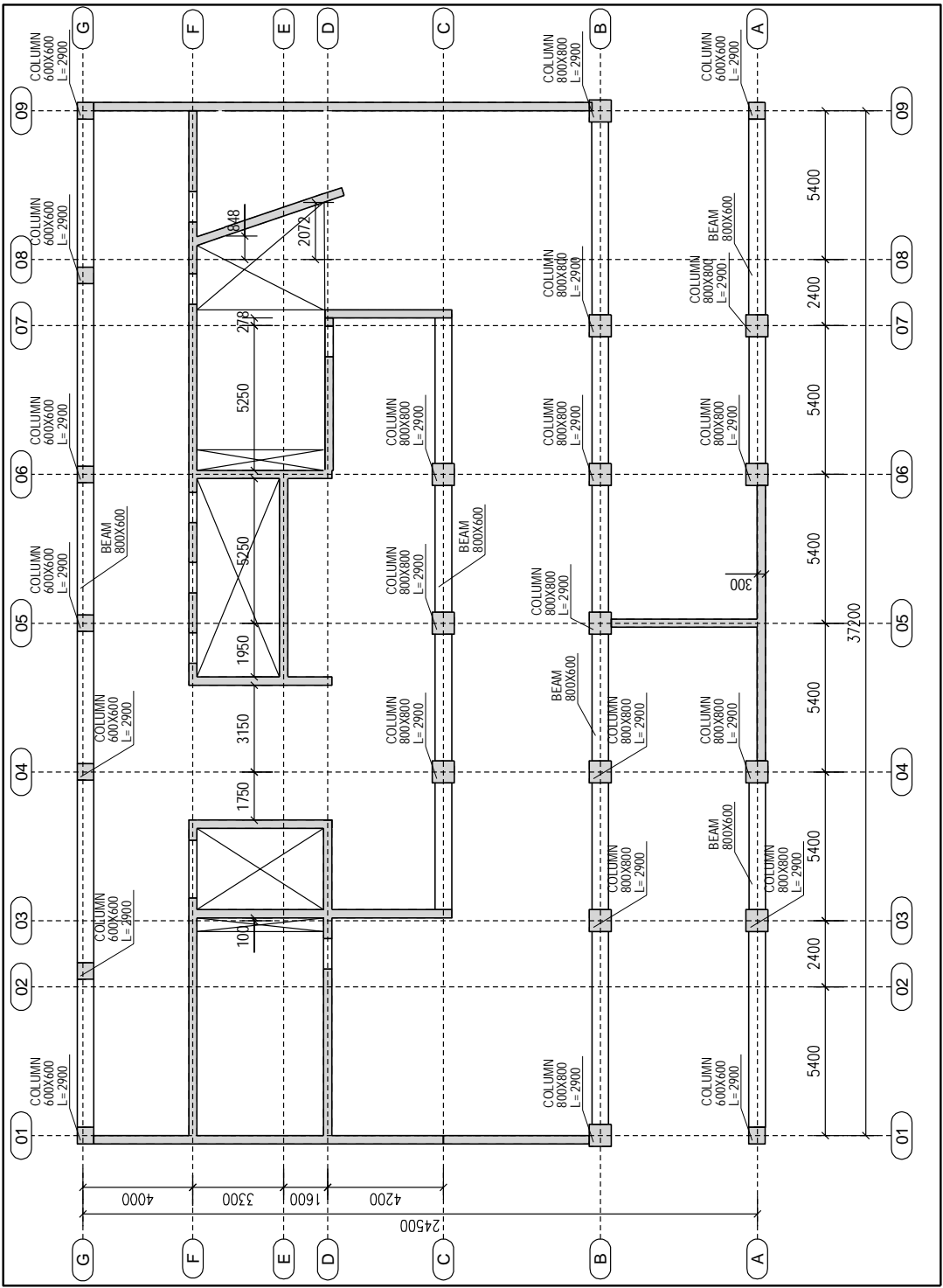
$$\text{Row 01} \quad \frac{f_1 + f_2 + f_3}{3} = 0.999$$

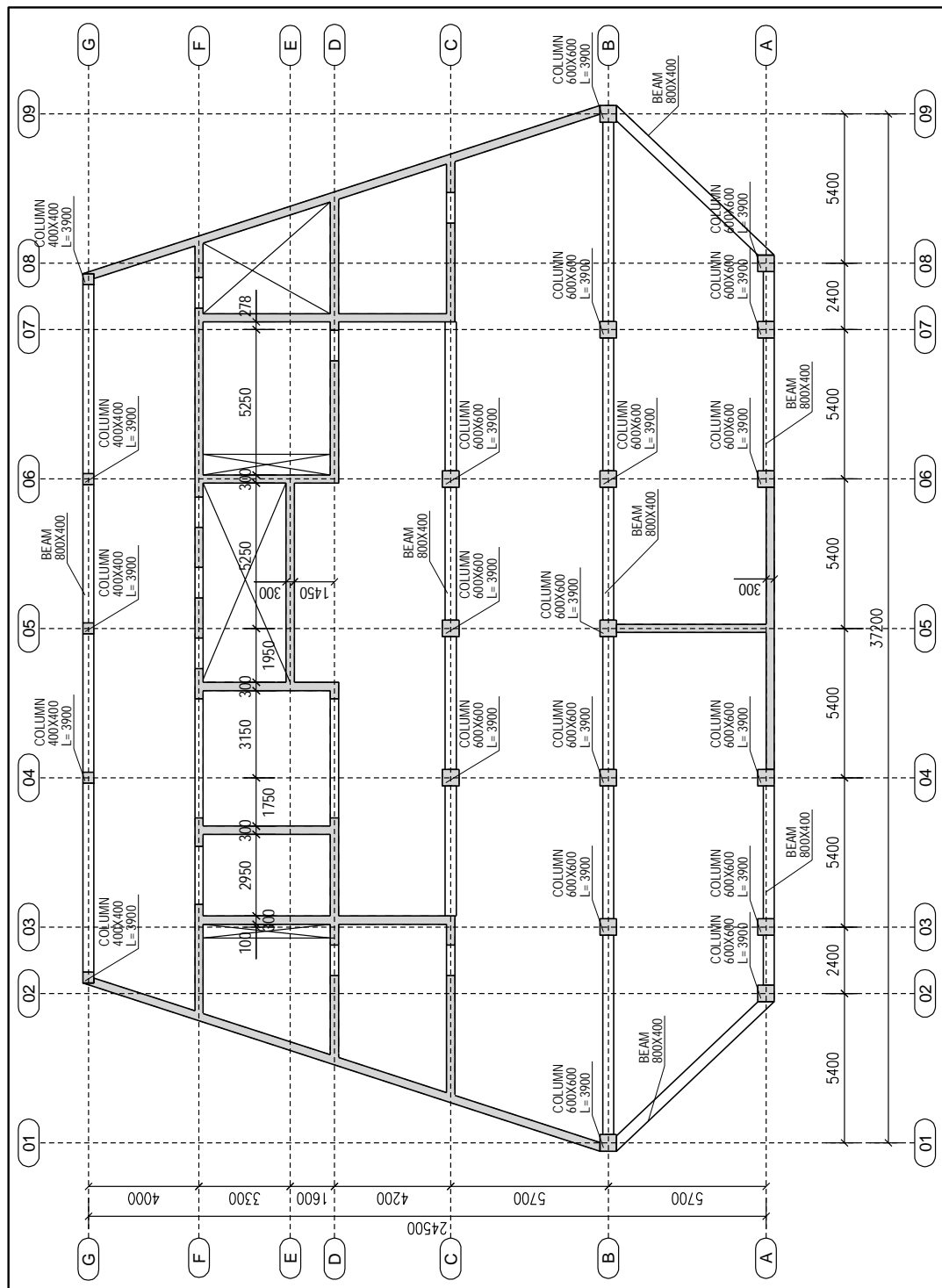
$$\text{Row 02} \quad \frac{f_4 + f_5 + f_6}{3} = 0.781$$

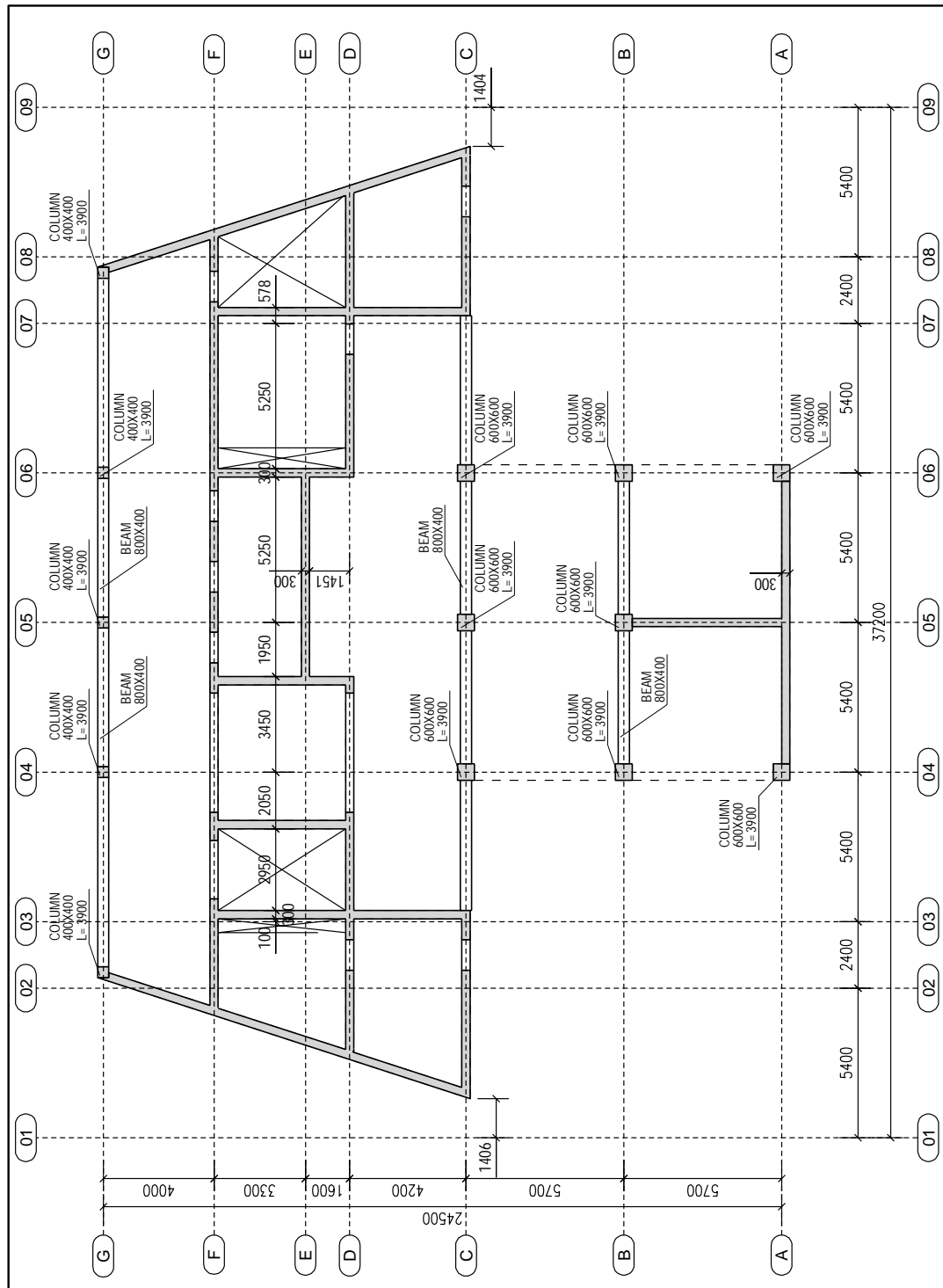
$$\text{Row 03} \quad \frac{f_7 + f_8 + f_9}{3} = 0.782$$

D Annex 04

Building model

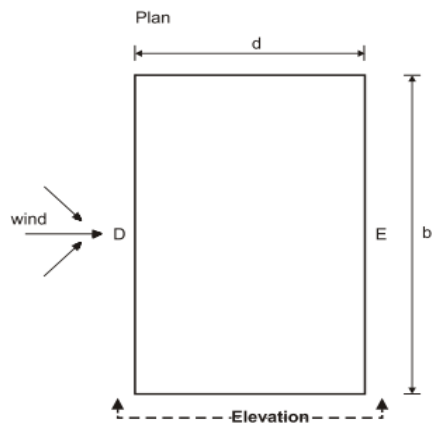
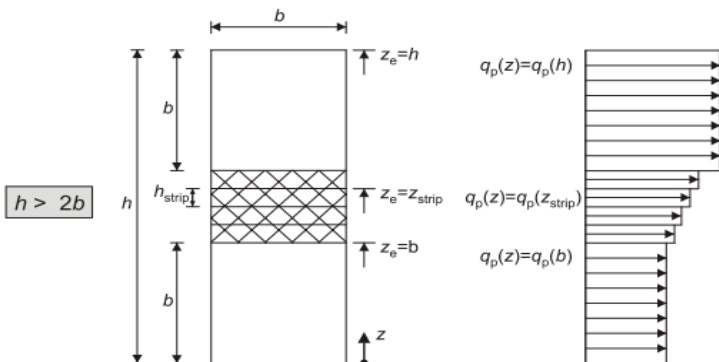






E Annex 05

Wind load calculations

Wind forces in "X" direction								
Terrain category	III	Basic wind velocity (V_b)	22 m/s					
Height of the building (h)	92,3 m	Terrain Factor (k_r)	0,2154					
Building face to the wind	37,2 m							
Along wind direction	22 m							
Fundamental mean velocity ($V_{b,0}$)	22 m/s							
Directional factor (C_{dir})	1							
Season factor (C_{season})	1							
Turbulence factor (k_t)	1							
Roughness length (z_0)	0,3 m							
Roughness length ($z_{0,II}$)	0,05 m							
Density of air (ρ_{wind})	1,25 kg/m ³							
Ration h/d		4,20						
Zone D $C_{pe,10}$		0,8						
Zone E $C_{pe,11}$		0,7						
								
height of building (m)		$C_r(z)$	$C_o(z)$	$V_m(z)$ (m/s)	$I_v(z)$	$q_p(z)$ (N/m ²)	$q_p(z)$ -D (kN/m ²)	$q_p(z)$ -E (kN/m ²)
2 parking + 7 floors $z \approx b \approx 37,2m$		34,9	1,0245	1,0	22,54	0,2102	784,76	0,628
$z_{strip}=4,1m \rightarrow z=z_i+z_{strip}$		39	1,0484	1,0	23,07	0,2054	810,67	0,649
$z_{strip}=4,1m \rightarrow z=z_i+z_{strip}$		43,1	1,0699	1,0	23,54	0,2013	834,29	0,667
$z_{strip}=4,1m \rightarrow z=z_i+z_{strip}$		47,2	1,0895	1,0	23,97	0,1977	856,00	0,685
$z_{strip}=4,1m \rightarrow z=z_i+z_{strip}$		51,3	1,1075	1,0	24,36	0,1945	876,10	0,701
$z_{strip}=4,1m \rightarrow z=z_i+z_{strip}$		55,4	1,1240	1,0	24,73	0,1916	894,84	0,716
last 9 floors $z \approx b \approx 22m$		92,3	1,2340	1,0	27,15	0,1746	1023,41	0,819

Wind forces in "Y" direction									
Terrain category	III	Basic wind velocity (V_b)		22 m/s					
Height of the building (h)	92,3 m	Terrain Factor (k_r)		0,2154					
Building face to the wind	22 m								
Along wind direction	37,2 m								
Fundamental mean velocity ($V_{b,0}$)	22 m/s								
Directional factor (C_{dir})	1								
Season factor (C_{season})	1								
Turbulence factor (k_t)	1								
Roughness length (z_0)	0,3 m								
Roughness length ($z_{0,II}$)	0,05 m								
Density of air (ρ_{wind})	1,25 kg/m ³								
Ration h/d									2,48
Zone D $C_{pe,10}$		0,8							
Zone E $C_{pe,11}$		-0,7							
height of building (m)		$C_r(z)$	$C_o(z)$	$V_m(z)$ (m/s)	$I_v(z)$	$q_p(z)$ (N/m ²)	$q_p(z)$ -D (kN/m ²)	$q_p(z)$ -E (kN/m ²)	
2 parking + 4 floors $z \approx b \approx 22m$		22,6	0,9309	1,0	20,48	0,2314	686,71	0,549	-0,481
$z_{strip}=4,1m \rightarrow z=z_i+z_{strip}$		26,7	0,9668	1,0	21,27	0,2228	723,70	0,579	-0,507
$z_{strip}=4,1m \rightarrow z=z_i+z_{strip}$		30,8	0,9976	1,0	21,95	0,2159	756,01	0,605	-0,529
$z_{strip}=4,1m \rightarrow z=z_i+z_{strip}$		34,9	1,0245	1,0	22,54	0,2102	784,76	0,628	-0,549
$z_{strip}=4,1m \rightarrow z=z_i+z_{strip}$		39	1,0484	1,0	23,07	0,2054	810,67	0,649	-0,567
$z_{strip}=4,1m \rightarrow z=z_i+z_{strip}$		43,1	1,0699	1,0	23,54	0,2013	834,29	0,667	-0,584
$z_{strip}=4,1m \rightarrow z=z_i+z_{strip}$		47,2	1,0895	1,0	23,97	0,1977	856,00	0,685	-0,599
$z_{strip}=4,1m \rightarrow z=z_i+z_{strip}$		51,3	1,1075	1,0	24,36	0,1945	876,10	0,701	-0,613
$z_{strip}=4,1m \rightarrow z=z_i+z_{strip}$		55,4	1,1240	1,0	24,73	0,1916	894,84	0,716	-0,626
$z_{strip}=4,1m \rightarrow z=z_i+z_{strip}$		59,5	1,1394	1,0	25,07	0,1890	912,38	0,730	-0,639
$z_{strip}=4,1m \rightarrow z=z_i+z_{strip}$		63,6	1,1538	1,0	25,38	0,1867	928,88	0,743	-0,650
$z_{strip}=4,1m \rightarrow z=z_i+z_{strip}$		67,7	1,1672	1,0	25,68	0,1845	944,47	0,756	-0,661
$z_{strip}=4,1m \rightarrow z=z_i+z_{strip}$		71,8	1,1799	1,0	25,96	0,1826	959,23	0,767	-0,671
las 5 floors $z \approx b \approx 22m$		92,3	1,2340	1,0	27,15	0,1746	1023,41	0,819	-0,716

F Annex 06

Pile distribution

